N 71 10373
CR 111098

EAST HARTFORD, CONNECTICUT

Report J-910900-6

Analytical Studies of In-Reactor Tests of a Nuclear Light Bulb Unit Cell

NASA Contract SNPC-70

CASE FILE COPY

UNITED AIRCRAFT CORPORATION

United Aircraft Research Laboratories

EAST HARTFORD, CONNECTICUT

United Aircraft Research Laboratories

UNITED AIRCRAFT CORPORATION

EAST HARTFORD, CONNECTICUT

Report J-910900-6

Analytical Studies of In-Reactor Tests
of a Nuclear Light Bulb Unit Cell

NASA Contract SNPC-70

REPORTED BY Thomas S. Latham
Thomas S. Latham

Harold E. Bauer
Harold E. Bauer

APPROVED BY James W. Clark
James W. Clark, Chief
Fluid and Systems Dynamics

DATE September 1970

NO. OF PAGES 82

COPY NO. 27

FOREWORD

An exploratory experimental and theoretical investigation of gaseous nuclear rocket technology is being conducted by the United Aircraft Research Laboratories under Contract SNPC-70 with the joint AEC-NASA Space Nuclear Propulsion Office. The Technical Supervisor of the Contract for NASA is Captain C. E. Franklin (USAF). Results of portions of the investigation conducted during the period between September 16, 1969 and September 15, 1970 are described in the following eight reports (including the present report) which comprise the required first Interim Summary Technical Report under the Contract:

1. Klein, J. F. and W. C. Roman: Results of Experiments to Simulate Radiant Heating of Propellant in a Nuclear Light Bulb Engine Using a D-C Arc Radiant Energy Source. United Aircraft Research Laboratories Report J-910900-1, September 1970.

2. Jaminet, J. F. and A. E. Mensing: Experimental Investigation of Simulated-Fuel Containment in R-F Heated and Unheated Two-Component Vortexes. United Aircraft Research Laboratories Report J-910900-2, September 1970.

3. Vogt, P. G.: Development and Tests of Small Fused Silica Models of Transparent Walls for the Nuclear Light Bulb Engine. United Aircraft Research Laboratories Report J-910900-3, September 1970.

4. Roman, W. C.: Experimental Investigation of a High-Intensity R-F Radiant Energy Source to Simulate the Thermal Environment in a Nuclear Light Bulb Engine. United Aircraft Research Laboratories Report J-910900-4, September 1970.

5. Bauer, H. E., R. J. Rodgers and T. S. Latham: Analytical Studies of Start-Up and Dynamic Response Characteristics of the Nuclear Light Bulb Engine. United Aircraft Research Laboratories Report J-910900-5, September 1970.

6. Latham, T. S. and H. E. Bauer: Analytical Studies of In-Reactor Tests of a Nuclear Light Bulb Unit Cell. United Aircraft Research Laboratories Report J-910900-6, September 1970. (present report)

7. Palma, G. E. and R. M. Gagosz: Optical Absorption in Transparent Materials During 1.5 Mev Electron Irradiation. United Aircraft Research Laboratories Report J-990929-1, September 1970.

8. Krascella, N. L.: Analytical Study of the Spectral Radiant Flux Emitted from the Fuel Region of a Nuclear Light Bulb Engine. United Aircraft Research Laboratories Report J-910904-1, September 1970.

Report J-910900-6

Analytical Studies of In-Reactor Tests of a Nuclear Light Bulb Unit Cell

TABLE OF CONTENTS

	Page
SUMMARY	1
RESULTS AND CONCLUSIONS	2
INTRODUCTION	4
CANDIDATE NUCLEAR TEST REACTORS	5
Pewee and the Nuclear Furnace	5
The High Flux Isotope Reactor (HFIR)	6
UNIT CELL CONCEPTUAL DESIGN	7
Basic Configuration	7
Alternate Configurations	8
GENERAL PERFORMANCE ANALYSIS	10
Reference Design Performance Levels	14
Selection of Fuel Partial Pressure	16
COMPONENT DESIGN	18
Pressure Vessel	18
Reflective Liner	19
Coolant and Buffer Gas Systems	19
Fuel Handling System	20
Assembly of In-Reactor Test Unit	21

TABLE OF CONTENTS (Continued)

Page

SIMULATION EXPERIMENTS IN THE UARL 1.2-MEGW R-F HEATER. 24

Comparison of Performance Levels 24
Future Simulation Experiments. 25

PERFORMANCE MEASUREMENTS. 26

Flow Measurements 26
Temperature Measurements 27
Spectral Measurements. 27
Post-Test Inspection 28

RECOMMENDATIONS FOR FUTURE RESEARCH 29

REFERENCES. 30

LIST OF SYMBOLS 32

TABLES. 35

FIGURES 43

Report J-910900-6

Analytical Studies of In-Reactor Tests of a Nuclear Light Bulb Unit Cell

SUMMARY

Analytical studies were conducted to determine the performance and design characteristics of a small model of a nuclear light bulb unit cell suitable for testing in a nuclear reactor. Three nuclear test reactors were considered: Pewee and the Nuclear Furnace, which are solid-core nuclear rocket fuel element test reactors, and the High Flux Isotope Reactor (HFIR). These test reactors have thermal neutron flux levels in the test region which range from 2.0 to 5.0 x 10^{15} neutrons/cm^2-sec. Demonstration tests with these thermal neutron flux environments would create thermal radiation fluxes corresponding to black-body radiating temperatures of 12,500 to 14,600 R for models having reflecting walls and operating pressures of 500 atm.

Preliminary design analyses of the test region pressure vessel, reflective liner, fuel handling system, and instrumentation were performed. Three types of tests of increasing complexity were considered: (1) a demonstration that nuclear fuel can be contained fluid dynamically while fissioning in a gaseous cloud; (2) a demonstration that internally cooled transparent walls are capable of withstanding both the nuclear radiation and thermal environments anticipated for a nuclear light bulb engine; and (3) a demonstration that seeded propellant can be heated to exhaust temperatures in excess of those presently attained in the solid-core nuclear rocket.

The results of the analytical study indicate that meaningful in-reactor demonstration tests of fuel containment, transparent-wall performance, and propellant heating could be conducted. In addition, it appears that the models could be thoroughly developed and tested using the UARL r-f induction heater and d-c arc facilities at performance levels similar to those anticipated for in-reactor demonstration tests.

RESULTS AND CONCLUSIONS

1. A reference test configuration with the following principal characteristics was selected: (1) test region diameter, D_T = 3.15 in.; (2) test region length, L_T = 8.40 in.; (3) U-235 fuel injected in the form of submicron particles; (4) argon buffer gas; (5) fuel-to-test region radius ratio, R_F/R_T = 0.6; (6) test region pressure, P_T = 500 atm; (7) average pressure of nuclear fuel within the fuel cloud, $\bar{P}_{F6}$ = 167 atm; and (8) surface reflectivity of inner periphery of test region, $\mathcal{R}$ = 0.9.

2. The test performance calculated for this configuration on the basis of a thermal neutron flux level of 2.5 x 10^{15}n/cm^2-sec was as follows: (1) mass of nuclear fuel in test region, M_F = 8.3 g of U-235; (2) average thermal neutron fission cross section, $\bar{\sigma}_f$ = 323 barns; (3) total test region power level, Q_T = 456 Btu/sec; (4) net radiated heat flux, Q_R/S_F = 1190 Btu/sec-ft^2 (8.81 kw/sq in.); (5) equivalent black-body radiating temperature, T* = 7040 R; (6) outward thermal radiating flux of 11,900 Btu/sec-ft^2 (88.1 kw/sq in.) and inward reflected flux of 10,710 Btu/sec-ft^2 (79.5 kw/sq in.) (difference equals net radiated heat flux, Q_R/S_F = 1190 Btu/sec-ft^2 (8.81 kw/sq in.)); and (7) fuel surface radiating temperature, T_6 = 12,500 R.

3. Test performance could be increased by approximately a factor of two by employing Pu-239 fuel instead of U-235. The average thermal neutron fission cross section for Pu-239 in the test region neutron flux environment would be $\bar{\sigma}_f$ = 678 barns.

4. It would be feasible to place internally cooled, fused silica, transparent-wall configurations against the reflective aluminum liner and thereby expose them to both the nuclear radiation and thermal environments of the test region. The total thermal radiation energy flux (incident plus reflected) would be 22,610 Btu/sec-ft^2 (166 kw/sq in.) compared with 20,600 Btu/sec-ft^2 (151 kw/sq in.) for the reference nuclear light bulb engine.

5. It would be feasible to conduct in-reactor propellant heating demonstration tests. The addition of a propellant duct would require a reduction in the test cavity diameter to approximately 2.5 in. if the pressure vessel inner diameter remains constant. The effects of the addition of the propellant heating duct on the unit cavity operating conditions have not been determined. It would be preferable to perform fuel region and transparent-wall in-reactor tests before attempting propellant heating demonstrations.

6. It was concluded that test region pressures up to 500 atm could be contained within a fiberglass pressure vessel employing heat-resistant phenolic resin binder to prevent deterioration of the pressure vessel strength due to thermal and radiation environments. The pressure vessel can be adequately cooled by the hydrogen coolant flowing past the outer periphery of the pressure vessel. Pressure vessel end walls were designed to be reusable to allow replacement of the fiberglass pressure vessel when the radiation dosage reaches 5×10^9 rads ($\sim$ 50 percent of the dosage level at which tensile strength begins to deteriorate). It is estimated that each pressure vessel could be used for 1 to 2 hours of full-power operation of the test reactor.

7. A highly polished reflective aluminum liner could be fabricated which would have an average surface reflectivity of $\mathcal{R} = 0.90$. This reflectivity is based upon a black-body spectrum at 12,500 R with corrections for surface area lost to end-wall injection and thru-flow exhaust duct areas.

8. Nuclear fuel would be injected in the form of a particle-carrier-gas mixture. The fuel system would include a spent-fuel scrubber and collector system. Experimental research is required to determine the fuel-to-carrier gas mass flow ratios achievable and the geometry and flow conditions required to remove spent fuel from the vortex region with minimum deposition of nuclear fuel in the exhaust ducts.

9. Heat balance measurements throughout the system could be made with flow-meters and thermocouples similar to the instruments employed in the solid-core nuclear rocket development program. Instruments to view the fissioning plasma to obtain spectral data could be developed through experimental research employing the UARL r-f induction heater.

10. Simulation of the performance conditions estimated for in-reactor demonstration tests could be performed using the UARL 1.2-megw r-f induction heater and d-c arc facilities.

INTRODUCTION

The present emphasis in the nuclear light bulb (Ref. 1) feasibility research being conducted under Contract SNPC-70 is to demonstrate radiant heating of a simulated propellant by transmitting energy through internally cooled transparent-wall models using arc-heated and r-f-heated plasmas as the energy source for the thermal radiation. A next possible major step in the development of a nuclear light bulb engine, assuming successful results from the arc and r-f experiments, is a series of demonstrations in which the arc- or r-f-heated plasma is replaced by a fissioning gas as the energy source for thermal radiation.

The principal requirement for a nuclear test reactor in which to perform demonstration tests is that it have a sufficiently high power-density and thermal neutron flux level to cause vaporization of nuclear fuel in the test cell. An additional requirement is that a test site, such as a beam port or flux trap, on the order of 3 to 5 in. in diameter be available. A review of candidate nuclear test reactors has indicated that Pewee or the Nuclear Furnace (solid-core nuclear rocket fuel element test reactors) and the High Flux Isotope Reactor (HFIR) are all well suited for in-reactor demonstration experiments.

The major objectives of the present investigation were directed toward (1) the preliminary design of the principal components of a unit cell for in-reactor demonstration tests, (2) identification of candidate test reactors, (3) prediction of the performance levels of selected test configurations, (4) conceptual design of a fuel handling system, (5) determination of the complexity of initial demonstration tests, and (6) identification of test parameters to be measured and the types of instrumentation required.

CANDIDATE NUCLEAR TEST REACTORS

The performance of in-reactor demonstration tests of a nuclear light bulb unit cell requires a high-power-density nuclear test reactor which can provide thermal neutron fluxes of sufficient magnitude to create a fissioning plasma in the gaseous fuel region. In addition, it is estimated that the test site (such as a beam port or flux trap) to accommodate the unit cell should be from 2 to 5 in. in diameter with access from both ends if at all possible. Finally, the frequency of operation of the test reactor should be high enough to run several tests a year. Three candidate test reactors with the requisite power densities, thermal neutron fluxes, and possible test sites to accommodate the unit cell were considered. These reactors are Pewee and the Nuclear Furnace, designed by Los Alamos Scientific Laboratory (LASL) to test solid-core nuclear rocket fuel elements, and the High Flux Isotope Reactor (HFIR) at the Oak Ridge National Laboratory (ORNL). Unit cell demonstration tests could be performed in a Pewee reactor, but the run times and frequency of operation (runs of one hour in duration about once every 18 months) seriously restrict flexibility in performing different types of tests. The test reactor which currently offers the greatest potential in flexibility of design and testing frequency appears to be the Nuclear Furnace. However, the construction and operation of the Nuclear Furnace is dependent upon the funding level and pace of development for the solid-core nuclear rocket. HFIR, as an alternative test reactor, is currently operating and should continue to be considered as a potential test reactor for unit cell demonstration tests.

Pewee and the Nuclear Furnace

Discussions have been held with staff members of LASL to explore the feasibility of inserting a unit cell in a Pewee reactor. Assembly drawings, a one-dimensional model for nuclear analysis, and neutron cross sections were supplied by LASL to provide a starting point for determining the characteristics of an in-reactor demonstration test. Results of studies in which the nuclear environment in test sites in the Pewee reactor were calculated are reported in Ref. 2. There are two test sites of interest in Pewee; a centrally located flux trap and the reflector region. Both test sites would accommodate a unit cell about 3.0 in. in diameter. The thermal neutron flux in these sites could be as high as 3.0×10^{15} n/cm^2-sec. The average thermal neutron fission cross sections for U-235 and Pu-239 were calculated to be 323 and 678 barns, respectively, in either test location. The Pewee reactors also have good hydrogen coolant handling facilities which could be employed in demonstration tests. The principal disadvantage of the Pewee reactors is the operating schedule.

The Nuclear Furnace is a light-water-moderated test reactor designed for the same purpose as Pewee; the testing of solid-core nuclear rocket fuel elements. It will be a smaller reactor and more flexible with regard to run schedules and design changes to accommodate unit cell demonstration tests. The light-water should develop a softer thermal neutron spectrum and therefore cause slight changes in the average thermal neutron fission cross sections for both U-235 and Pu-239. However, for purposes of this study, it was assumed that the Nuclear Furnace can provide the same neutron flux environment as that calculated for Pewee and, due to its design flexibility, can accommodate a unit cell up to 4.0 in. in diameter.

The High Flux Isotope Reactor (HFIR)

The High Flux Isotope Reactor (HFIR) at ORNL has several test sites which could accommodate a unit cell test configuration. These test sites are described in Ref. 3 and are listed below.

Test Site	Inside Diameter	Thermal Neutron Flux
Central Flux Trap	5.0 in.	3.0 to 5.0 x 10^{15} n/cm^2-sec
Horizontal Beam Tubes In Beryllium Reflector	4.0 in.	3.0 to 5.0 x 10^{14} n/cm^2-sec
Engineering Facility Tubes In Beryllium Reflector	3.5 in.	10^{14} n/cm^2-sec

The average thermal neutron fission cross section in the test sites for U-235 is $\bar{\sigma}_f = 385$ barns. The principal advantage of HFIR is that it operates continuously during its core lifetime of 23 days. There is about one day of down-time to load a new core between runs. Testing in the HFIR reactor would most likely interrupt the isotope production schedule and would therefore require careful coordination and scheduling with strict limitations on the number of tests which could be run.

UNIT CELL CONCEPTUAL DESIGN

The conceptual design of a unit cell for in-reactor tests consists of a cylindrical cavity in which the conditions of a single unit cavity of a nuclear light bulb engine would be simulated. This unit cell could be inserted in a nuclear test reactor to examine the characteristics of such a cell in a nuclear environment. The in-reactor tests would be an intermediate step between the electrically heated unit cell tests performed with the d-c-arc or r-f-heated plasmas and full-scale engine tests. It would permit investigation of nuclear-heated vortexes and studies of the effects of operation in a nuclear reactor environment. The basic configuration would consist of a cylindrical cavity with highly reflecting walls. Modifications to the basic configuration could be made to include transparent walls inside the reflecting walls and to permit propellant heating experiments.

Basic Configuration

The basic design configuration of the unit cell for the in-reactor tests is a cylindrical cavity with an inside diameter of 3.15 in. and a length of 8.4 in. The cylinder is made of aluminum with a highly reflecting inner surface. Flow channels to provide for the injection of buffer gas, fuel and the required coolants for the components are provided, and the entire assembly is contained in a fiberglass pressure vessel. A sketch of the assembly is shown in Fig. 1. The outside diameter of the pressure vessel is approximately 3.85 in. so that the entire assembly could be inserted in a 4-in.-dia test port in an existing reactor. Variations of these dimensions may be required, depending on the size of the access ports available in the test reactor selected for the experiments or the size of the cavity configuration required to achieve the performance levels of the tests. The basic design would remain the same for these dimensional variations.

A sectional view of the basic configuration is shown in Fig. 2. The cavity region is formed by a cylinder with an inside diameter of 3.15 in. and a wall thickness of 0.0625 in., and two end walls which are also 0.0625-in. thick. The coolant and fuel injection ducts are formed by a series of concentric cylinders. Beginning from the cavity centerline, the flow circuits are: (1) the fuel injection tube; (2) the inner bypass flow annulus; (3) the outflow port; (4) the outer bypass flow annulus; (5) the end-wall coolant outlet; (6) the end-wall coolant inlet; and (7) the liner coolant annulus. The region between the end-wall coolant outlet and inlet (ducts (5) and (6)) is not used for coolant flow and this region may be used for measuring or monitoring devices. The sketch in Fig. 2 is approximately full scale and indicates the amount of space which would be available for instrumentation in this region.

The total length of the in-reactor test unit is dependent upon the reactor used for the tests. It is preferred that the unit be long enough so that the pressure vessel end caps can be located away from high neutron or gamma-ray fluxes. The end caps and high-pressure fittings require a large mass of metal which would have to be internally cooled if they are exposed to an intense radiation flux. Estimates of the actual length required for use in typical test reactors indicate an overall length of the unit on the order of 6 ft.

Alternate Configurations

A number of alternate configurations have been considered, including configurations with fuel injection ports in the end wall off the cavity centerline, and configurations which would permit the testing of transparent walls and propellant heating. These alternate configurations use basically the same type of coolant flow circuitry and do not introduce any major modifications to the basic unit design or assembly procedures.

Alternate Location of Fuel Injection Ports

Fluid dynamics tests to determine the best location for fuel injection ports are in progress. If it is determined that it is better to inject fuel at some location in the end wall other than the cavity centerline, the relocation of the fuel injection port simplifies the test unit configuration. A sketch of an in-reactor test unit with off-center fuel injection ports is shown in Fig. 3. In this configuration, the outflow from the cavity region exits through a tube rather than an annulus, as in Fig. 2, and only one bypass flow annulus is required. The cooling requirements and operating conditions are essentially the same as in the basic configuration.

Tests of Different Complexity

The basic configuration is designed primarily for the study of the effects of the nuclear environment, the characteristics of the vortex region and the fuel handling problems. With modification, the basic configuration may be adapted to permit the inclusion of transparent structures and propellant heating regions.

Experiments with transparent structures can be conducted by inserting a transparent-wall model in the cavity adjacent to the cavity liner as shown in Fig. 4(a). The modifications required for these tests would be: (1) extension of the buffer-gas injectors to inject the buffer gas tangent to the inner transparent wall; (2) inclusion of piping and manifolding for the internal coolant in the transparent structure; and (3) additional instrumentation, as required, to indicate the operating conditions in the transparent structure. Feeder manifold pipes for the transparent structure could be located in the cavity as shown in Fig. 4(a) if they were also transparent.

Investigations of propellant heating in an in-reactor test would require modifications to the cavity liner and necessitate a decrease in the cavity inside diameter if the pressure vessel is not changed. One possible configuration is shown in Fig. 4(b). In this configuration, a section of the liner is moved out approximately 0.75 in. so that the cavity is formed by a section of reflecting liner and a section of transparent wall as shown. The propellant heating region is formed by the transparent wall and sections of reflecting liner wall. The problems of supporting the transparent wall would be simplified by the configuration shown since the transparent-wall feeder and collector pipes and the buffer-gas injectors could be located behind the inner sections of the reflecting liner rather than being supported by struts as in the reference engine. In this configuration it is necessary to include piping and manifolding for the transparent-wall coolant and provisions for the injection and removal of the simulated propellant gas. All of the additional piping and instrumentation can be accomodated in the region between the liner and the pressure vessel.

The modifications necessary to accomodate propellant heating tests entail major changes in the test unit configuration. Because of the increased complexity of these tests, and the major modifications of the unit heat balance which would be caused by the inclusion of a seeded propellant channel, it is recommended that a series of tests of the base unit, with and without transparent walls, be performed before attempting to conduct propellant heating tests. The propellant duct, as shown in Fig. 4(b), will introduce an asymmetric heat sink which may change the conditions in the vortex and could cause changes in the operating conditions in the cavity. Tests of propellant heating using the d-c arc heater, such as those reported in Ref. 4 and future tests which are scheduled which employ an asymmetric propellant duct should give some indication of the effects of these asymmetric configurations. The d-c arc tests will also be used to refine the design of an in-reactor propellant heating test configuration and to determine the performance levels required in the test unit.

If the driving reactor selected for the tests has an accessibility that would permit a number of test per year, a test schedule involving a series of unit cavity and transparent-wall tests prior to the propellant heating tests could be completed in a reasonable length of time.

GENERAL PERFORMANCE ANALYSIS

The determination of the performance levels expected in an in-reactor demonstration test involves a combination of analytical predictions of flow conditions and heat balance and the incorporation of experimentally measured parameters. The experimentally measured parameters are related principally to fuel containment factors such as average fuel residence time, fuel region radius, and fuel-to-buffer gas density and partial pressure ratios.

Flow conditions for the argon buffer gas were determined by the methods employed in Ref. 1 for the full-scale engine. The axial velocity, v_Z, was determined to be that required for the region between the edge of the fuel and the peripheral wall of the test chamber to be two viscous boundary layers thick, 2δ, using the conditions at the edge of the fuel region as reference conditions. Thus, from Ref. 1

$$\delta = \frac{R_1 - R_6}{2} = 2.4 \left[\frac{\mu_6}{\rho_{B_6}} \frac{L_T/2}{v_Z} \right]^{1/2} \tag{1}$$

The viscosity, μ_6, and density, ρ_{B6}, of the argon buffer gas varies with the edge-of-fuel temperature, T_6. The argon viscosities employed for these analyses were taken from Ref. 5.

As in Ref. 1, it was assumed that the axial dynamic pressure was constant between the edge of the fuel cloud and the peripheral chamber wall. Assuming the temperature in the buffer gas varies linearly in this region, it is possible to obtain an expression for the local axial velocity by assuming $\rho_B v_Z^2/2g$ = constant. The weight flow of the buffer gas can be expressed by

$$W_B = \int_{R_6}^{R_1} 2\, \rho_B v_Z \, dA \tag{2}$$

The next step in the analysis requires the incorporation of experimental results from both heated and isothermal two-component gas vortex tests. The mass of nuclear fuel which can be contained in the test cell can be expressed by

$$M_F = k_F\, \rho_{B_6} V_T \tag{3}$$

where k_F is an experimentally measured containment parameter. The containment parameter, k_F, is given by

$$k_F = \bar{\rho}_{F_1} / \rho_{B_6} \tag{4}$$

where $\bar{\rho}_{F_1}$ is the fuel density averaged over the entire vortex chamber volume, V_T. The most recently measured range for this parameter given in Ref. 6 is $k_F = 0.1$ to 0.4. This range of values was employed in the in-reactor test performance analysis.

Another measured parameter, c, is required to estimate the fuel injection flow rate, W_F, which is given by

$$W_F = \frac{M_F}{c\,\tau_B} \tag{5}$$

where τ_B is the average buffer-gas residence time in the vortex chamber and c is the ratio of average fuel-to-buffer-gas residence times. The average buffer-gas residence time is given by

$$\tau_B = \frac{V_B}{W_B}\,\bar{\rho}_B \tag{6}$$

where V_B is the buffer-gas region volume and $\bar{\rho}_B$ is the average buffer-gas density. $\bar{\rho}_B$ is calculated from the expression

$$\bar{\rho}_B = \int_{R_6}^{R_1} \frac{\rho_B L_T \, dA}{V_B} \tag{7}$$

The measured values from Ref. 6 of the average residence time ratio, c, range from 0.5 to 1.5. This range of values was also employed in the in-reactor test performance analyses.

To obtain a heat balance for the unit cell, it is necessary to calculate the rates of energy loss by radiation, conduction, and convection and equate the sum of these to the energy generation rate due to fissioning of the nuclear fuel.

The energy radiated from a nuclear fuel cloud which is optically thick (fuel cloud diameter equal to many photon mean-free-paths) is given by

$$Q_R = \sigma \left[T^{*4} S_F - T_W^{\,4} S_W \right] \tag{8}$$

where T^* is the equivalent black-body radiating temperature of the fuel region, σ is the Stefan-Boltzmann constant ($\sigma = 0.48 \times 10^{12}$ Btu/sec-ft^2-deg R). S_F and S_W are the fuel and wall surface areas respectively, and T_W is the chamber wall temperature ($T_W = 1000$ R). The fuel-region surface area, S_F, is related to another measured quantity, the ratio of fuel-to-cavity radius, R_F/R_T. This ratio varied from 0.5 to 0.9 in the experiments reported in Ref. 6. For purposes of these analyses, R_F/R_T was varied from 0.6 to 0.8.

One of the possible experiments which might be performed in an in-reactor test would be to place internally cooled transparent walls such as those envisioned for the full-scale engine near the unit cell inner surface and expose them to the combined nuclear and thermal radiation environments. A high photon flux could be created by lining the cavity walls with polished aluminum with a reflectivity of $\mathcal{R} = 0.9$ averaged over the wavelength range encompassing the photons emitted from the hot fuel cloud. In that case, the fuel region surface radiating temperature, T_6, would be increased by the factor $[1/(1-\mathcal{R})]^{1/4} = 1.78$, (i.e., to provide a net outflow of radiant energy of one unit, the true gross outflow must be 10 units to make up for the reflection of 9 units back toward the fuel). The equivalent fuel-region black-body radiating temperature, T^*, corresponds then to a net radiant heat flux which is a tenth of the gross outward radiated heat flux. Note however, (see Ref. 7), that the true edge-of-fuel temperature for zero reflectivity is slightly less than T^* and, for finite reflectivity, is slightly less than T_6.

The energy conducted away from the fuel cloud is given by

$$Q_{COND} = K \frac{\Delta T}{\Delta R} S_F \tag{9}$$

where K is the thermal conductivity of argon buffer gas at the edge-of-fuel temperature, T_6. Thermal conductivity values for argon were taken from Ref. 5.

The energy convected away from the test region by the flowing buffer gas and fuel is given by

$$Q_{CONV} = W_B C_{P_B} \Delta T_B + \frac{3}{2} W_F C_{P_F} \Delta T_F \tag{10}$$

Since the argon and fuel have approximately equal values for specific heat, the fuel weight flow was assumed to be 3/2 times the value calculated in Eq. (5) to include the buffer gas in the fuel region. The buffer gas temperature rise, ΔT_B, is calculated from

$$\Delta T_B = \overline{T}_B - T_W \tag{11}$$

where $\overline{T}_B$ is the temperature of argon of an average density of $\overline{\rho}_B$ from Eq. (7) for the operating pressure level. The fuel temperature rise, ΔT_F, is given by

$$\Delta T_F = 3T^* - T_W \tag{12}$$

where the assumption that the average fuel temperature is approximately three times the radiating temperature is implied.

The total rate of energy release, Q_T, the sum of the individual energy release rates, is equated to the rate of fission energy release by

$$Q_T = Q_R + Q_{COND} + Q_{CONV} = \gamma N_F \overline{\sigma}_f \phi_{th} V_F \tag{13}$$

where γ is a constant of proportionality, N_f is the nuclear fuel atom density, $\overline{\sigma}_f$ is the average thermal neutron fission cross-section, and ϕ_{th} is the thermal neutron flux. In evaluating the constant of proportionality, γ, it was assumed that the

energy release per fission was 175 Mev. This level of energy release per fission takes credit for energy deposition in the fuel cloud from only fission fragments and a small fraction of beta particle and gamma radiation.

Calculations to determine temperature distribution in the fuel-containment region of gaseous nuclear rocket engines based on the transfer of energy by thermal radiation from the fuel to the propellant were reported in Ref. 8. Temperature distributions were determined for two sets of fuel opacities based on two sets of theoretical estimates of fuel ionization potentials (Refs. 9 and 10). Figure 5 was constructed from the data contained in Ref. 8 and shows the effect of fuel partial pressure on the average fuel density for different amounts of radiative heat transfer per unit length of fuel cloud. The results shown in Fig. 5 are based on a diffusion theory analysis of radiation transport in the fuel region and are valid for situations in which the photon mean-free-path is many times smaller than the fuel region diameter, which is the case for the in-reactor test configuration under consideration. The curves in Fig. 5 were used to obtain fuel partial pressures in the fuel region for calculated fuel densities and radiated energy per unit length of fuel cloud.

The equations discussed above were programmed for digital computer solution to evaluate the performance of in-reactor test configurations over wide ranges of thermal neutron fluxes and operating conditions. The results of these performance calculations are described in the following section.

Reference Design Performance Levels

A reference unit cell with an inside diameter of 3.15 in. and a length of 8.40 in. was selected for preliminary performance analyses and preliminary component design. The operating pressure level was set at 500 atm, the pressure level envisioned for the full-scale nuclear light bulb reference engine. Initially, the effects on performance due to variations of principal parameters such as thermal neutron flux level, unit cell diameter, fuel-containment factor, aluminum liner reflectivity, and fuel-to-cavity radius ratio were calculated. Specific reference parameters and operating conditions were selected from these results. The selected values or ranges of values for the parameters affecting the performance of the reference unit cell are listed in Table I.

The variations of power radiated and effective black-body radiating temperature with thermal neutron flux level for the reference unit cell are shown in Fig. 6. The two sets of curves correspond to two different values of $\bar{\sigma}_f$, the average thermal neutron fission cross-section. A value of $\bar{\sigma}_f$ = 323 barns was calculated for U-235 in the reflector of the Pewee reactor. The same value of $\bar{\sigma}_f$ = 323 barns will be assumed for the Nuclear Furnace and HFIR, recognizing that this assumption may be

conservative since light-water moderation will develop a softer thermal neutron spectrum and hence, a slightly higher average fission cross-section (for example, $\bar{\sigma}_f = 385$ barns in the HIFR flux trap). Pu-239 has a calculated average fission cross-section of $\bar{\sigma}_f = 678$ barns in the Pewee reflector. Again, the same value will be assumed for Pu-239 in the Nuclear Furnace and HFIR. The ranges of thermal neutron fluxes available in the Nuclear Furnace, Pewee, and HFIR are shown in Fig. 6. For purposes of further performance analyses, the thermal neutron flux was held constant at $\phi_{th} = 2.5 \times 10^{15}$ n/cm^2-sec. This level of neutron flux was chosen because it represents a value attainable in any of the three candidate test reactors.

Ranges of power levels and radiating temperatures over a wide variation of fuel partial pressures are shown in Fig. 7 for the two values of average fission cross-section considered. Thermal neutron flux was fixed at $\phi_{th} = 2.5 \times 10^{15}$ n/cm^2-sec for the results shown in Fig. 7. An average fuel partial pressure of $\bar{P}_{F6} = 167$ atm was selected for the reference design performance level. A value of $\bar{P}_{F6} = 250$ atm (i.e., $\bar{P}_{F6}/P_T = 0.5$) represents an upper limit on containment achieved in the two-component vortex experiments reported in Ref. 6 for the reference design fuel-to-cavity radius ratio of $R_F/R_T = 0.6$. The reference design performance level was selected for the case in which U-235 fuel was employed with an average fission cross-section of $\bar{\sigma}_f = 323$ barns. The principal performance parameters and operating conditions for the reference design case are listed in Table II. A substantial increase in performance can be achieved by using Pu-239 with an average fission cross-section of $\bar{\sigma}_f = 678$ barns. For purposes of comparison, in-reactor test performance for the reference design unit cell with substitution of Pu-239 for U-235 is also shown in Table II.

Several of the parameters affecting performance were varied individually while all other reference conditions were held constant to determine the sensitivity of the performance level to these parameters. The quantities varied were unit cell diameter, aluminum liner reflectivity, fuel-containment factor, and the fuel-to-cavity radius ratio. The resulting effects on performance levels due to variations in these selected parameters are shown in Fig. 8. The greatest variations in performance result from changes in unit cell diameter and the fuel-containment factor (see Figs. 8(a) and (b)) principally because these parameters have a direct effect on the amount of nuclear fuel stored in the test cell. Note that when unit cell diameter is varied, the cell length-to-diameter ratio is held constant such that the fuel region volume increases as the cube of the diameter. Variation of the aluminum liner reflectivity (Fig. 8(c)) has a large effect on the gross outward photon flux which is proportional to T_6^4. The slight rise in radiated power as the aluminum liner reflectivity decreases results from an increase in stored nuclear fuel because the buffer gas-density at the edge of the fuel cloud, ρ_{B6}, increases (note that the density containment factor, $\bar{\rho}_{F1}/\rho_{B6}$, is held constant in this case). For purposes of testing internally cooled transparent-wall models and propellant heating, it is desirable to have high gross outward photon fluxes and therefore,

a reflectivity of $\mathcal{R} = 0.9$ was chosen as the reference design value. Performance is shown to be relatively insensitive to changes in fuel-to-cavity radius ratio in Fig. 8(d). This relative insensitivity is due to the constraint that the density containment factor, $\bar{\rho}_{F_1}/\rho_{B_6}$, is held constant and is independent of fuel-region radius. Since the equivalent black-body radiating temperature, T^*, varies as $(S_F)^{1/4}$ under these conditions, there is little variation in the êdge-of-fuel temperature and buffer-gas density, T_6 and ρ_{B_6}, and hence little resultant variation in stored nuclear fuel as the fuel-to-cavity radius ratio is changed over the range from $R_F/R_T = 0.6$ to 0.9. A fuel-to-cavity radius ratio of $R_F/R_T = 0.6$ was chosen as a reference design condition to minimize fuel concentrations near the test cell aluminum liner.

Selection of Fuel Partial Pressure

The fuel partial pressure selected for the reference design performance level was chosen to fall within the limits of experimental results from two-component gas vortex tests. Table III contains comparisons of typical partial-pressure ratios measured in the experiments reported in Ref. 6 and the partial-pressure ratios selected for the in-reactor tests. It can be seen that, in all cases, the values chosen for the in-reactor tests are less than those reported for the measurements of Ref. 6.

In the case of the reference design performance level, the partial pressure selected for the nuclear fuel affects the fuel-to-carrier-gas mass flow rate ratio required for fuel injection. For the fuel-to-total-pressure ratio of $\bar{P}_{F_6}/P_T = 0.33$ ($\bar{P}_{F_6} = 167$ atm), a peak local pressure ratio in the fuel region of $P_F/P_T = 0.50$ would be required. This value was determined by observing that the peak-to-average fuel pressures measured in the simulated fuel region in the experiments of Ref. 6 were about $P_{F_{max}}/\bar{P}_{F_6} = 1.5$. These pressure ratios are for the nuclear fuel only, hence $P_{F_{max}} = 250$ atm in the reference design in-reactor test. When carrier gas is employed, the carrier-gas partial pressure, P_{CG}, must be added to that of the fuel (i.e., it too must be considered as fuel for purposes of estimating the total partial pressure in the fuel region due to gases other than the buffer gas). Local fuel partial pressures higher than $P_F/P_T = 0.75$ were obtained in the experiments described in Ref. 6. If this value of local partial pressure, $(P_{F_{max}} + P_{CG})/P_T = 0.75$ is selected as an upper limit for the in-reactor tests, then within the fuel region, $P_{F_{max}} + P_{CG} = 375$ atm and $P_{F_{max}}/P_{CG} = 2.0$. In the case of the reference performance, the nuclear fuel is, on the average, singly ionized and the electrons are included in the total partial-pressure taken from Fig. 5. Therefore, since approximately half of the fuel partial pressure for the reference design performance level is due to electrons, the ratio of uranium atom-to-carrier-gas partial pressure can be reduced to $P_U/P_{CG} = 1.0$. These average and peak values of partial pressures in the fuel region for the reference design in-reactor tests are summarized as follows:

Constituent	Average Partial Pressures, atm	Partial Pressures at Point of Peak Fuel Concentration, atm
U and U^+	83.3	125.0
Electrons	83.3	125.0
Carrier Gas (Argon)	83.4	125.0
Buffer Gas (Argon)	250.0	125.0
Total	500.0	500.0

When argon with an atomic weight of 40 is employed as the carrier gas, the injected mass flow rate ratio of fuel-to-carrier gas required to limit $P_U/P_{CG} \geqq 1.0$ must be $W_F/W_{CG} \geqq 6.0$.

COMPONENT DESIGN

The discussion of the design of the components in the in-reactor test unit is subdivided into five parts, (1) the pressure vessel, (2) the reflective liner and end walls, (3) the fuel handling system, (4) the coolant and buffer-gas systems, and (5) the procedures to be followed in assembling the components. The component descriptions apply only to the basic design configuration, and the dimensions given are for a unit similar in size to that described in Ref. 2.

Pressure Vessel

The pressure vessel used in the in-reactor test is a wound fiberglass cylinder approximately 6 ft in length with an inside diameter of 3.5 in. and an outside diameter of 3.85 in. The wall thickness of 0.175 in. is based on an internal pressure of 500 atm and a design stress level of 75,000 psi in the fiberglass. The maximum allowable uniaxial tensile stress for fiberglass is on the order of 300,000 psi. If it is assumed that the pressure vessel is wound so that it has similar tensile stress properties in both axial and hoop stress (alternate circumferential and axial fiber directions or 45-deg angle winding), the maximum allowable stress would be reduced to 150,000 psi. This value was further reduced to the design level quoted above to provide a safety factor of 2.0. A type of winding which yields equal values of allowable hoop and axial stress was selected so that the cross-sectional area reductions in the fiberglass which are required to provide for metallic end pieces would not require increases in the outside diameter of the vessel. In a cylinder under an internal hydrostatic load, the ratio of hoop stress to axial stress is 2 to 1. Therefore, a 50 percent reduction in thickness of the fiberglass to accommodate the metal end pieces may be made.

The pressure vessel is cooled on both sides so that the maximum-allowable temperature of 700 R will not be exceeded at the values of neutron and gamma-ray heating which are anticipated at full-power operation of the test reactor.

The resin which is used in the fabrication of fiberglass components is degraded by exposure to radiation as discussed in Ref. 11. Total operating lifetimes are on the order of 1 to 3 hours depending upon the neutron and gamma-ray flux levels in the particular test reactor to be used. The other components of the in-reactor test unit are not limited by radiation exposure, and a design which would permit replacement of the pressure vessel is preferred.

Reflective Liner

The cavity liner and end walls of the in-reactor test cell (Fig. 2) are made from aluminum with a highly reflecting inner surface. The heat deposited in these components, as given in Table IV, is removed by hydrogen coolant. The liner coolant passes axially between the outer surface of the liner and the inner surface of the pressure vessel. The end-wall coolant enters the test region through an annulus at the outer edge of the end wall, passes radially inward, and is removed through an annulus near the axial centerline as shown in Fig. 2. The maximum allowable temperature in the liner or end wall was taken as 1400 R. The specifications and operating conditions of the cavity liner and end walls are given in Table V.

The portion of the end walls which form the ends of the bypass coolant annuli (Fig. 2) cannot be cooled by the end-wall coolant, and these regions must be transpiration cooled with a small portion of the bypass coolant. The portion of the end wall which forms the end of the inner bypass flow annulus is separated from the remainder of the end walls by the outflow annulus, and it is necessary to support this region by means of struts located in the outflow annulus. These supports must be located in the annulus downstream of the mixing region so that they will not be exposed to the hot gases leaving the vortex.

Coolant and Buffer Gas Systems

A schematic diagram of the in-reactor test flow circuits is shown in Fig. 9. The flow circuits are symmetric about the axial centerline of the unit, and also symmetric about the cavity mid-plane with the exception of the liner coolant, which is a single-pass circuit. The annuli which form the flow circuits are shown in Fig. 2 and the operating conditions in the various circuits are listed in Table VI.

The buffer gas enters the cavity through four axial tubes (Fig.2) and is injected into the vortex through a series of holes which are tangent to the inner surface of the liner. The tube inside diameter necessary to maintain a reasonable pressure loss (about 2 atm) in the buffer-gas inlets is 0.10 in. The annulus between the liner and pressure vessel was fixed at 0.110 in. to provide sufficient space for the buffer-gas injector tubes.

Hydrogen coolant was selected for use in the basic in-reactor test configuration because the primary coolant for the driving reactor assumed for this study (Pewee reactor) is hydrogen. If the unit were employed in a water-cooled driving reactor the flow circuits could be redesigned for use with water without major modification of the unit.

Fuel Handling System

A fuel injection system which minimized the partial pressure of non-fissioning gases in the unit cell fuel region, namely a particle-carrier-gas system, was selected for the in-reactor test reference design. Factors considered in the design of a fuel handling system employing particle-carrier-gas mixtures were (1) fuel-to-carrier-gas mass flow ratios required, (2) heating of the nuclear fuel during injection, (3) fuel particle lifetimes upon injection into the unit cell, (4) methods of removal of the spent-fuel, fission fragments, and buffer gas from the test region, and (5) systems for collecting spent-fuel and fission fragments.

The minimum required fuel-to-carrier-gas flow rate ratio for injection into the unit cell is established by the peak fuel partial pressure required for the reference design performance level. That flow rate ratio was calculated in a previous section entitled Selection of Fuel Partial Pressure to be $W_F/W_{CG} \geqq 6.0$ Development of systems to achieve particle-to-carrier-gas weight flow ratios of $W_F/W_{CG} \geqq 6.0$ should be the objective of future experimental research programs.

Heating of the fuel during injection will occur when the fuel is exposed to the neutron flux of the driving reactor. The unit cell length is 8.4 in. and the core lengths of the driving reactors may be considerably larger. Therefore, the fuel will be exposed to the neutron flux of the driving reactor for one or two feet prior to injection, assuming that the test cavity is centered in the reactor. The fission heating rates are extremely high (24,800 Btu/sec-lb) due to the high neutron flux levels in the driving reactors, and calculations were made of the total temperature rise in the fuel during injection as a function of injection tube diameter. The results of these calculations indicated that it would be necessary to reduce the fission heating rates in the injection tubes by means of neutron-absorbing coatings on the injection tubes if injection temperatures on the order of 1000 R were to be maintained. It was assumed that the fuel injection tube would be made from a neutron absorbing material such as cadmimum or Boral (50-percent boron carbide, 50-percent aluminum by weight) so that the fission heating rate would be reduced to approximately 248 Btu/sec-lb. With these heating rates and two 0.024-in.-dia injection tubes (one in each end wall) the fuel injection temperatures would be approximately 900 R. The calculated pressure loss in a 3-ft length of the injection tube was 1 atm.

The lifetime of both U-235 and Pu-239 particles upon injection into the fuel region was calculated by dividing the total enthalpy rise required to vaporize U-235, initially at room temperature (1150 Btu/lb (Ref. 12)), by the rate of energy release per pound of nuclear fuel for the reference design thermal neutron flux level of $\phi_{th} = 2.5 \times 10^{15}$ n/cm^2-sec. This resulted in vaporization times of 4.6×10^{-2} and 2.23×10^{-2} sec for U-235 and Pu-239, respectively. It was assumed that the vaporization of Pu-239 would require the same total enthalpy rise as that for U-235. These lifetimes are about two orders of magnitude shorter than the reference design average fuel residence-time of $\tau_F = 3.5$ sec.

A mixture of fuel, fission fragments, carrier gas, and buffer gas is removed from the cavity through an annular outflow port in each end wall. The temperature of this mixture is on the order of 8000 R prior to leaving the cavity and, therefore, the mixture must be rapidly cooled and isolated from the walls of the outflow port. The cooling of the mixture is achieved by injecting a flow of relatively cold argon gas through the walls of the outflow duct. The injection geometry for the bypass flow must be designed to both protect the duct walls and to initiate condensation of the entrained fuel to a solid particle form while minimizing the possibility of fuel deposition on the duct wall. The required geometric configuration has not been determined, but experimental investigations of this problem will be undertaken. The amount of bypass flow necessary to reduce the mixed mean temperature of the mixture exiting the cavity and the bypass flow to below the melting point of uranium (2500 R) is 1 lb/sec. This flow enters through two annuli surrounding the outflow annulus and is injected in the cavity end-wall region.

The mixture of fission products, spent-fuel, and argon buffer and carrier gas can be ducted into a water injection scrubber. Water could be injected in sufficient quantity to drop the exit temperature below the boiling point of water. Subsequent centrifuging would separate the water carrying most of the uranium and fission products from the argon gas. The water and argon gas would be collected in leak-tight containers for subsequent separation and purification. Such a scrubber-collector system would not be large since, for a typical run time of 1000 sec, the total masses of argon and uranium passed through the fuel-containing test region would be 7.8 and 5.3 lb, respectively.

Assembly of In-Reactor Test Unit

The in-reactor test unit consists of a series of concentric cylinders which form annular flow passages for the various coolant circuits. The majority of the unit operates at a relatively low temperature (less than 1200 R) and is constructed from aluminum. The bypass flow channels and the outflow annulus may be subjected to temperatures of up to 2500 R and must be constructed from a high-temperature material such as inconel. Although the entire assembly operates at approximately 500 atm, there is no requirement for high-pressure seals between the flow circuits in the unit. The aluminum-to-aluminum joints may be made by brazing, and the inconel parts may be welded. Where it is necessary to form a connection between inconel and aluminum, a mechanical connection may be used. In the following discussion of the assembly procedure, the sequence in which the various parts are joined is outlined but the exact method of joining is not specified.

The in-reactor test unit is divided into three major sub-assembles in the following discussions: (1) the liner, (2) the end-wall and coolant ducts, and (3) the end cover plates. The assembly sequence for each sub-assembly is discussed and the sequence of joining the major sub-assemblies is described.

Liner Assembly

The liner is an aluminum cylinder with a highly reflective inner surface. The argon buffer-gas is injected tangent to the inner wall through a series of injectors located in four axial rows. These injectors are fed by four buffer-gas injector pipes which are located in the annulus between the liner and the pressure vessel. The four buffer-gas injector pipes are attached to the liner as shown in Fig. 10. Flow enters from both ends of the buffer-gas injector pipes and passes through the liner wall to the inner surface.

End-Wall and Coolant Ducts

The cavity end wall is aluminum with a highly reflecting inner surface. Provision must be made for the injection of fuel, removal of buffer flow, end-wall cooling and bypass flow injection. These flow circuits are formed by a series of concentric annuli which must be assembled starting with the innermost walls. Sketches of the assembly at the inner and outer ends are shown in Figs. 11 and 12, respectively.

The innermost tube is the fuel-injection tube. This tube is attached to the end walls as shown in Fig. 11. The inner bypass flow annulus is formed by the fuel-injection tube and a concentric wall which is also attached to the end wall as shown in Fig. 11. At the outer end (see Fig. 12) a flange is used to connect the two concentric tubes and form a closed flow passage for the inner bypass flow. The bypass flow is injected into the annulus at the outer end by one or more feeder pipes which are attached to the flange as shown in Fig. 12. This sub-assembly is separated from the remainder of the end wall by the outflow duct and it must be supported by spacer bars which position the sub-assembly as shown in Fig. 11.

The outer bypass flow annulus is formed by attaching two concentric cylinders to the remaining portion of the end wall as shown in Fig. 11. The outer ends of these annuli are also closed and feeder pipes attached as shown in Fig. 12. At this time, the fuel tube and inner bypass tube sub-assembly are inserted and attached to the outer bypass tube sub-assembly at the outer end only, thereby forming the outflow annulus. The end-wall coolant passages are formed by inserting an annular baffle assembly between the outer bypass flow annulus wall and the outer section of the liner. This baffle assembly is formed by two cylinders with flanges on the outer

end as shown in Figs. 11 and 12. The baffle sub-assembly is positioned by spacer bars which locate the sub-assembly at the required distance from the end wall, outer liner, and outer bypass flow tube. This sub-assembly slides over the outer bypass flow tube and is attached to the outer bypass flow tube at the outer end only. The outer liner, which has the same dimensions as the liner in the cavity region, but does not require a highly reflecting inner surface, surrounds the other sub-assemblies, and is attached to the end wall (Fig. 11) and to the end-wall coolant baffle sub-assembly at the outer end. The location of the buffer-gas flow injectors is shown in Figs. 11 and 12, but these parts are not attached to these sub-assemblies. The end-wall and coolant duct assemblies are now attached to the cavity liner assembly by joining the cavity liner and cavity end walls.

End Cover Plates

The feeder tubes for fuel, coolants, buffer gas and bypass gas and the outlets for coolant and outflow are all attached to the central portion of the end cover plates as shown in Fig. 13. This inner portion of the cover plate is mechanically attached to the liners. The buffer-gas injector pipes pass through the liner to the central portion of the cover plate. The completed assembly may now be inserted in the pressure vessel.

The outer cover plate is used to connect the assembly to the ends of the pressure vessel as shown in Fig. 13. Fittings for connecting feeder and exhaust pipes are attached to the outer cover plate and all external piping must be designed to withstand the full 500 atm pressure which exists in the in-reactor test unit at operating conditions.

SIMULATION EXPERIMENTS IN THE UARL 1.2-MEGW R-F HEATER

A considerable amount of preliminary non-nuclear testing of the in-reactor test unit and its components can be performed using the 1.2-megw r-f heater to produce a radiation source. The discussion of the types of tests which could be performed is divided into two sections: (1) a comparison of the performance levels of the in-reactor test unit and the existing 1.2-megw r-f heater configuration, and (2) the modifications to the present r-f heater configuration which would permit the testing of full-scale in-reactor test units. In general, the type of experiments which could be performed include verification of analytical heat balance calculations, measurements of the reflectivity of various liner materials and surfaces and, with appropriate modifications, could include tests of full-scale models of in-reactor test units to identify any design problems which might exist prior to the start of nuclear testing of the units.

Comparison of Performance Levels

The calculated performance levels of the in-reactor test unit described in this report and the performance levels of the 1.2-megw r-f heater as employed in FY 1970 tests are shown in Table VII. The major differences between the two configurations arise from the difference in geometry and the operating pressure levels The r-f heater in its present configuration would accommodate tests of components of 2/3-scale relative to the diameter, but of a much shorter length. The values of radiant heat flux per unit area which have been obtained in the r-f heater are approximately 6 times as high as those anticipated in the in-reactor tests but these values were obtained with discharge diameters of 0.5 in. and discharge lengths of 2.0 in. If it is desired to increase the discharge volume to values closer to that calculated for the fuel region of the in-reactor test (1.9-in.-dia), the radiant heat flux levels for the same power level would be changed in inverse proportion to the surface area.

Increases in the diameter of the plasma discharge cause an increase in the ratio of plasma diameter to coil diameter which leads to higher coupling efficiency in the r-f heater. It should be relatively easy to obtain discharge power levels of 456 Btu/sec (432 kw), to simulate the U-235-fueled in-reactor test unit, and it may be possible to obtain discharge power levels approaching 840 Btu/sec (797 kw), to simulate the Pu-239-fueled in-reactor test unit, with the present 1.2-megw input capacity of the power supply. If higher power levels are required, the input power of the r-f heater may be increased to 2.4 megw by relatively simple changes to the power supply. Calculations indicate less of a problem with total radiated powers of 446 kw with a ratio of plasma diameter to coil diameter of 0.6 than with the 223 kw power level and 0.25 ratio of plasma-diameter-to-coil-diameter as employed in present r-f heater tests.

Even though the length of the present r-f heater is much smaller than that of the in-reactor test unit, a number of experiments on end-wall configurations to determine heat loads, reflectivity and desired end-wall geometry can be performed. Segments of cylindrical liner can also be tested in the r-f heater to study buffer-gas injection geometries and verify calculated heat loads.

Experiments to determine the characteristics of the fuel handling system could also be performed by injecting uranium into the argon plasma. These experiments would be used to determine injection and extraction methods which would minimize fuel deposition problems and also indicate any changes in the radiation spectrum which occur if uranium is present in the plasma.

Instrumentation proposed for the in-reactor tests, particularly in the instrumentation required for spectral emission measurements, could be checked during tests in the r-f heater.

Future Simulation Experiments

In order to perform the types of experiments described in the preceding section with a full-scale in-reactor test unit, it would be necessary to modify the resonator section of the r-f heater. The modifications necessary are (1) increases in size to accommodate a full-size in-reactor test unit (3.15-in.-dia, 8.4-in.-length), (2) increases in the operating pressure levels, and (3) modifications to permit operation with large-diameter discharges with high power levels. If it is possible to approximate the in-reactor test conditions in the r-f heater, complete non-nuclear tests of the in-reactor test unit can be made to include verification of heat balances, and preliminary tests of fuel handling systems and buffer-gas injection methods. Calibration of all of the instrumentation scheduled for the in-reactor tests could be made and the effectiveness of the measuring techniques investigated.

The use of the r-f heater with full-scale in-reactor units would make it possible to identify many problem areas which might exist in the unit prior to undertaking a nuclear test and should provide a high confidence level for successful nuclear tests of the unit.

PERFORMANCE MEASUREMENTS

The performance of the in-reactor test unit will be determined by measurement of the flow rates and temperatures in the various coolant circuits to determine the enthalpy change in each coolant, by spectral measurement of the radiant heat flux in the cavity and by post-test inspection of the components of the test unit. The flow circuits in the in-reactor test unit, as previously described, will permit separate measurements of the total heat deposited in the cavity liner, end walls, and in the mixture of fuel, fission products, buffer gas, and carrier gas which leaves the cavity region through the outflow port. It will be possible to calculate the contributions to neutron and gamma ray heating which are associated with the test reactor from those of the in-reactor test unit by operating an unfueled test unit in the reactor with the design coolant flow rates.

All of the measuring devices which are inside of the test unit must be of a type which are not subject to radiation damage at the radiation flux levels anticipated in the test unit at full-power operating conditions.

Flow Measurements

The flow rates in all of the coolant circuits and the buffer gas circuit may be measured with conventional flow metering equipment at a location external to the test unit. The liner coolant and end-wall coolant flow rates may be measured before they enter the test unit or after they exit the test unit since both circuits are separate, closed-loop circuits. The buffer gas, bypass flow and the fuel and carrier-gas flows must be measured before they enter the test unit since all of these flows are mixed before exiting through the outflow port. Total flow rates in the outflow port may be measured and compared with the sum of the buffer, bypass, fuel, and carrier-gas flows. A minimum of 13 flowmeters are required to monitor the various flow rates in the test unit.

Further analytical and experimental studies will be necessary to develop and test the equipment and techniques necessary to control and monitor the fuel flow rates if the fuel is injected in the form of particles in a carrier gas. Control of the fuel-to-buffer-gas ratio will be necessary to insure a consistent fuel and carrier-gas mixture for injection and adequate flow monitoring equipment must be available for the measurement of the fuel flow rate in both the fuel injection system and in the outflow port. It is possible to monitor the uranium flow rates in the unit test cell with alpha particle counters. This type of measurement is employed in the gaseous diffusion enrichment operations and can be used to detect very small uranium concentrations. The effects of fission product decay on the uranium flow measuring devices and the design of equipment required to produce a consistent ratio of fuel-to-carrier gas will require further studies.

Temperature Measurements

The temperature levels throughout the in-reactor test unit, with the exception of the internal cavity region, are below 2500 R and can be measured with conventional types of thermocouples. Monitoring of inlet and outlet temperatures in all of the coolant circuits is necessary to calculate the enthalpy rise in the circuits and the overall unit heat balance. In addition to these temperature measurements, it is necessary to monitor the temperature levels in the critical components such as the cavity liner, end walls, and pressure vessel to insure that the maximum allowable temperatures in these components are not exceeded. It is estimated that a minimum of 20 thermocouples will be required to provide sufficient information for the unit heat balance. These thermocouples would be located at the inlet and outlet of each coolant circuit and the measured temperature difference would indicate the enthalpy rise in that circuit. Provision must be made for sufficient insulation between separate coolant circuits to minimize heat transfer between the circuits if the heat load to a specific component is to be accurately determined. At least 10 additional thermocouples will be required to monitor component temperature levels through the unit.

Spectral Measurements

The spectral emission characteristics of the fuel region in the in-reactor test will require visual access to the fuel region. The light must be transmitted, through one or more light ducts, from the cavity region, which is at 500 atm, to an externally located monochromator. Light ducts from the end walls will pass directly through the region between the end-wall coolant annuli to the end cover plate. Light ducts from the cavity mid-plane will pass through the liner coolant annulus, parallel to the buffer-gas injection ducts and will require mirrors inside the light duct to bend the light to the location where the light duct penetrates the end cover plate. A window of some type will be required which is capable of withstanding the pressure differential but will not attenuate the radiation from the cavity. A glass or fused silica window will attenuate the ultraviolet (u-v) radiation but permit measurements in the visible spectrum: Some preliminary measurements of spectral emission characteristics of the plasma in the 1.2-megw r-f heater are described in Ref. 13 , Appendix B. It may be desirable to employ some form of aerodynamic window such as have been developed for lasers to permit transmission of the entire spectrum to the monochromator.

Spectral emission measurements will be made in the end-wall region of the cavity and also in the midplane region. The midplane location with a viewport in the liner wall would result in minimum attenuation due to the presence of fuel or fission fragments in the buffer layer.

Post-Test Inspection

The primary purpose of post-test inspection of the in-reactor test unit would be to determine if there were any erosion, corrosion, or fuel and fission fragment deposition problems in the test unit which did not cause noticeable changes in the performance levels during operation. In the event of a nonscheduled shutdown of the test unit, the post-test inspection would be required to determine the cause of the shutdown. The effects of nuclear radiation on the unit components, particularly the degradation in pressure-vessel strength, will also be determined by post-test pressure inspections. Destructive testing of the pressure vessel may be desired after initial tests to determine the amount of degradation in strength.

RECOMMENDATIONS FOR FUTURE RESEARCH

The basic in-reactor test configuration described in this report may require some modification based on the results of concurrent research and on the final selection of a driving reactor. These modifications will probably not require any changes in the basic geometric configuration but may require modifications to coolant flow rates or changes in the calculated performance levels.

Before the in-reactor test unit can be installed in a driving reactor, it will be necessary to determine the effects of the test unit on the driving reactor and to identify any possible personnel or reactor hazards associated with the in-reactor tests. This type of analysis will require an examination of the nuclear characteristics of the test unit with respect to the reactor used as a driving reactor and a preliminary analysis of the possible off-design operating conditions and possible failures which may occur during operation. It will also be necessary to determine the equipment and procedures required for removal, disassembly and inspection of the in-reactor test unit after nuclear tests.

In addition to the design studies mentioned above, a schedule of component fabrication and testing should be established to estimate the number and types of non-nuclear tests which should be performed prior to an in-reactor test. This schedule would aid in a determination of the required modifications to existing equipment which would be required to perform the desired non-nuclear testing and the sequence of testing needed to develop all of the components required for the tests.

Estimates of the costs of an in-reactor test program, including the costs of using various types of driving reactors, should also be made. These estimates should include a consideration of the operating times and accessability of various driving reactors and the reusability of in-reactor test components.

REFERENCES

1. McLafferty, G. H. and H. E. Bauer: Studies of Specific Nuclear Light Bulb and Open-Cycle Gaseous Nuclear Rocket Engines. United Aircraft Research Laboratories Report G-910093-37, prepared under Contract NASw-847, September 1967. Also issued as NASA CR-1030.

2. Latham, T. S.: Analytical Study to Determine the Characteristics of Nuclear Light Bulb Model Tests In A Pewee Reactor (U). United Aircraft Research Laboratories Report H-910375-5, prepared under Contract NASw-847, September 1969. (Confidential Restricted Data)

3. Benford, F. T., T. E. Cole, and E. N. Cramer: The High Flux Isotope Reactor. Oak Ridge National Laboratory Report ORNL-3572 (Rev. 2) Vols. 1A and 1B, June 1968.

4. Klein, J. F. and W. C. Roman: Results of Experiments to Simulate Radiant Heating of Propellant in a Nuclear Light Bulb Engine Using a D-C Arc Radiant Energy Source. United Aircraft Research Laboratories Report J-910900-1, prepared under Contract SNPC-70, September 1970.

5. Devoto, R. S.: Transport Coefficients of Partially Ionized Argon. The Physics of Fluids, Vol. 10, No. 2, February 1967, pp. 354-364.

6. Jaminet, J. F. and A. E. Mensing: Experimental Investigation of Simulated-Fuel Containment in R-F Heated and Unheated Two-Component Vortexes. United Aircraft Research Laboratories Report J-910900-2, September 1970.

7. Krascella, N. L.: Theoretical Investigation of Radiant Emission from the Fuel Region of a Nuclear Light Bulb Engine. United Aircraft Research Laboratories Report H-9109092-12, prepared under Contract NASw-847, September 1969.

8. Kesten, A. S. and N. L. Krascella: Theoretical Investigation of Radiant Heat Transfer in the Fuel Region of a Gaseous Nuclear Rocket Engine. United Aircraft Research Laboratories Report E-910092-9, prepared under Contract NASw-847. Also issued as NASA CR-695.

9. Williamson, H. A., H. H. Michels, and S. B. Schneiderman: Theoretical Investigation of the Lowest Five Ionization Potentials of Uranium. United Aircraft Research Laboratories Report D-910099-2, prepared under Contract NASw-847, September 1965.

10. Waber, J. T., D. Liberman, and D. T. Cromer: Unpublished Theoretical Ionization Potentials for Uranium. Los Alamos Scientific Laboratory, received June 1966.

REFERENCES (Continued)

11. Rittenhouse, J. B. and J. B. Singeltary: Materials for Space Stations. Metal Progress Vol. 89, No. 2, February 1966, pp. 56-63.

12. Katz, J. J. and E. Rabinowitch: The Chemistry of Uranium. Dover Publications, Inc., New York, 1951.

13. Roman, W. C.: Experimental Investigation of a High-Intensity R-F Radiant Energy Source to Simulate the Thermal Environment in a Nuclear Light Bulb Engine. United Aircraft Research Laboratories Report J-910900-4, September 1970.

LIST OF SYMBOLS

A	Area, ft^2
C	Ratio of average fuel residence-time to average buffer-gas residence-time
c_{p_B}	Specific heat of buffer gas, Btu/lb-deg R
c_{p_F}	Specific heat of fuel, Btu/lb-deg R
D_T	Unit cavity diameter, in.
g	Gravitational acceleration constant, ft/sec^2
k_F	Containment parameter
L_T	Unit cavity length, in.
M_F	Nuclear fuel mass, g
N_F	Nuclear fuel atom density, atm/cm^3
P_B	Partial pressure of buffer gas, atm
P_{CG}	Partial pressure of carrier gas, atm
$P_{F_{MAX}}$	Maximum partial pressure of fuel, atm
$\bar{P}_{F_6}$	Average fuel partial pressure, atm
P_T	Unit cavity operating pressure, atm
P_U	Partial pressure of uranium in cavity, atm
Q_{COND}	Conducted power, Btu/sec
Q_{CONV}	Convected power, Btu/sec
Q_R	Radiated power, Btu/sec
Q_T	Total power, Btu/sec

LIST OF SYMBOLS (Continued)

q_F	Heat flux from fuel region, Btu/sec-ft^2
$\mathcal{R}$	Reflectivity
R_1 or R_T	Unit cavity radius, ft
R_6 or R_F	Fuel region radius, ft
S_F	Fuel region surface area, ft^2
S_W	Unit cavity surface area, ft^2
$\bar{T}_B$	Average buffer-gas temperature, deg R
T_W	Cavity wall temperature, deg R
T_6	Temperature at edge of fuel region, deg R
T^*	Equivalent black-body radiating temperature, deg R
V_B	Buffer-gas region volume, ft^3
V_F	Fuel region volume, ft^3
v_Z	Axial velocity in buffer-gas region, ft/sec
W_B	Mass flow rate of buffer gas, lb/sec
W_{CG}	Carrier-gas mass flow rate, lb/sec
W_F	Fuel injection mass flow rate, lb/sec
γ	Proportionality constant
ΔT_B	Temperature rise in buffer gas, deg R
ΔT_F	Temperature rise in fuel, deg R
δ	Viscous boundary layer thickness, ft

LIST OF SYMBOLS (Concluded)

μ_6	Viscosity of edge of fuel, lb/ft-sec
ρ_B	Buffer-gas density, lb/ft^3
$\bar{\rho}_B$	Average buffer-gas density in volume between $R = R_1$ and $R = R_6$, lb/ft^3
ρ_{B6}	Buffer-gas density at edge of fuel ($R = R_6$), lb/ft^3
$\bar{\rho}_F$	Average fuel density, lb/ft^3
$\bar{\rho}_{F1}$	Average fuel density in volume between $R = 0$ and $R = R_1$, lb/ft^3
$\bar{\rho}_{F6}$	Average fuel density in volume between $R = 0$ and $R = R_6$, lb/ft^3
σ	Stefan-Boltzmann constant, 0.48×10^{-12} Btu/sec-ft^2-deg R
$\bar{\sigma}_f$	Average thermal neutron cross-section, barns
τ_B	Average buffer-gas residence-time, sec
τ_F	Average fuel residence-time, sec
ϕ_{th}	Thermal neutron flux, neutrons/cm^2-sec

TABLE I

VALUES SELECTED FOR PARAMETERS AFFECTING
IN-REACTOR TEST PERFORMANCE
Specifications For Unit Cell Shown In Figs. 1 and 2

Parameter	Range of Values	Reference Value
Operating Pressure, P_T - atm	--	500
Unit Cell Diameter, D_T - in.	2.0 - 4.0	3.15
Thermal Neutron Flux, ϕ_{th} - n/cm^2-sec	10^{14} - 5.0×10^{15}	2.5×10^{15}
Average Fission Cross-Section, $\bar{\sigma}_f$-barns	323 (U-235) 678 (Pu-239)	323
Fuel-to-Cavity Radius Ratio, R_T/R_F	0.6 - 0.8	0.6
Density Containment Factor, $\bar{\rho}_{F_6}/\rho_{B6}$	0.1 - 0.4	0.23
Ratio of Average Fuel Residence-Time to Buffer-Gas Residence-Time, τ_F/τ_B	0.5 - 1.5	1.0
Aluminum Liner Reflectivity, $\mathcal{R}$	0.7 - 0.9	0.9
Fuel-to-Buffer-Gas Partial-Pressure Ratio, $\bar{P}_{F_6}/P_B$	--	0.33

TABLE II

PERFORMANCE LEVELS OF IN-REACTOR TESTS
Specifications For Unit Cell Shown In Figs. 1 and 2

Operating Pressure, P_T = 500 atm
$\bar{\rho}_{F_1}/\rho_{B_6} \leqq 0.25$, $\bar{P}_{F_6} = P_T/3$, $R_F/R_T = 0.6$
Argon Buffer Gas

	Reference Design Performance	Performance Using Pu-239 Fuel
Fuel	U-235	Pu-239
Thermal Neutron Fission Cross-Section, $\bar{\sigma}_f$ barns	323	678
Surface Reflectivity $\mathcal{R}$	0.9	0.9
Density Containment Factor, $k_F = \bar{\rho}_{F_1}/\rho_{B_6}$	0.23	0.22
Fuel Loading, M_F - g	8.3	7.2
Total Power, Q_T - Btu/sec	456	840
Power Radiated, Q_R - Btu/sec	411	756
Surface Radiating Temperature, T_6 - deg R	12,500	14,600
Equivalent Black-Body Radiating Temperature, T* - deg R	7040	8210
Average Fuel Partial Pressure For Volume Inside R_6, $\bar{P}_{F_6}$ - atm	167	167

TABLE III

COMPARISON OF FLOW AND CONTAINMENT PARAMETERS FROM
TWO-COMPONENT GAS VORTEX EXPERIMENTS AND
VALUES SELECTED FOR IN-REACTOR TEST REFERENCE DESIGN
See Ref. 6 For Description of Two-Component Gas Vortex Experiments

Containment Parameter	Two-Component Gas Vortex Test	In-Reactor Test Reference Design
Density Containment Factor, $k_F = \bar{\rho}_{F_1}/\rho_{B_6}$	0.1 - 0.4	0.23
Ratio of Fuel-to-Buffer-Gas Residence-Times, $c = \tau_F/\tau_B$	0.5 - 1.5	1.0
Fuel-to-Cavity Radius Ratio, R_F/R_T	0.5 - 0.9	0.6
Fuel-to-Buffer-Gas Partial-Pressure Ratio, $\bar{P}_{F_6}/P_B$	0.1 - 0.5	0.33
Peak-to-Average Fuel Partial-Pressure Ratio, P_F/P_{F_6}	1.5	1.5

TABLE IV

UNIT CELL HEAT BALANCE
(See Fig. 2 for Details of Unit Cell Geometry)

Heat Balance Calculated For Reference Design Employing U-235 Fuel
Numbers In Parentheses Are For Pu-239 Fuel With Similar Flow Rates And Geometry

Energy Removed From Cavity, Btu/sec	
Radiation and Convection to Liner	336 (645)
Radiation and Convection to End Walls	64 (120)
Conduction and Convection to Buffer Flow	56 (75)
Total Energy from Fuel Region	456 (840)
Energy Removed in Coolant Flow Circuits, Btu/sec*	
Liner Coolant	341 (650)
End-Wall Coolant	34 (124)
Buffer Gas and Bypass Flow	62 (81)
Total Energy Removed by Coolant	471 (855)

*Includes Neutron and Gamma-Ray Heating of Components, 15 (15) Btu/sec.

TABLE V

LINER AND END-WALL SPECIFICATIONS
(See Figs. 1 and 2 for Details of Unit Cell Geometry)

Liner and End-Wall Material	Aluminum
Reflectivity of Inner Surface	0.90
Liner Outside Diameter, in.	3.275
Liner Inside Diameter, in.	3.15
Liner Total Length, in.	8.65
Maximum Temperature in Liner, deg R	949 (1364)*
End-Wall Thickness, in.	0.0625
Maximum End-Wall Temperature, deg R	900 (1248)

*Specifications calculated for reference design employing U-235 fuel. Numbers in parentheses are for Pu-239 fuel with similar flow rates and geometry.

TABLE VI

COOLANT AND BUFFER-GAS SYSTEM CONDITIONS
(See Figs. 1 and 2 for Details of Unit Cell Geometry)

Liner Coolant Flow Rate, lb/sec	2.0
Liner Coolant Annular Width, in.	0.110
Radiant Heat Load to Liner, Btu/sec	336 (645)*
Coolant Inlet Temperature, deg R	500
Temperature Rise in Hydrogen Liner Coolant, deg R	48 (93)
Film Temperature Difference in Liner, deg R	291 (561)
Wall Temperature Difference Across Liner, deg R	110 (210)
Maximum Temperature in Liner, deg R	949 (1364)
Pressure Loss in Liner Coolant Circuit, atm	5.88**
Hydrogen Coolant Flow Rate in Each End Wall, lb/sec	0.50
Radiant Heat Flow to Each End Wall, Btu/sec	33.5 (62)
Temperature Rise in Hydrogen End-Wall Coolant, deg R	19.5 (35.5)
Maximum Film Temperature Difference in End-Wall Region, deg R	267 (500)
Temperature Difference Across End Wall, deg R	132 (248)
Maximum Temperature in End Wall, deg R	900 (1248)
Pressure Loss in End-Wall Coolant Circuit, atm	4.04**

* Specifications calculated for reference design employing U-235 fuel. Numbers in parenthesis are for Pu-239 fuel with similar flow rates and geometry.

**Pressure losses based on 12 ft of length to include entrance and exit piping.

TABLE VI (Concluded)

Fuel-Injector Tube Inside Diameter, in.	0.024
Fuel-Injector Tube Outside Diameter, in.	0.108
Fuel Flow Rate per Tube, lb/sec	0.00265
Argon Carrier-Gas Flow Rate per Tube, lb/sec	0.000441
Fission Heating Rate in Fuel, kw/gm	58 (123)*
Fuel Injection Temperature, deg R	926 (1252)**
Argon Buffer-Gas Flow Rate, lb/sec	0.0635 (0.0725)
Bypass Argon Flow Rate, lb/sec	1.0
Temperature of Fuel and Buffer-Gas Mixture Exiting Cavity, deg R	8350 (9400)
Inlet Temperature of Bypass Flow, deg R	500
Temperature of Inner Bypass Flow at Injection, deg R	1501 (1720)
Temperature of Outer Bypass Flow at Injection, deg R	1736 (1933)
Mixed Mean Temperature of Fuel, Buffer and Bypass Flow, deg R	2030 (2380)
Temperature of Fuel, Buffer and Bypass Flow at Outlet of Active Core Region, deg R	1281 (1245)
Mass of Fuel in Cavity, g	8.3 (7.2)

*Heat generation in fuel injectors reduced by factors of 100 by addition of neutron absorbing material in tube walls.

**Specifications calculated for reference design employing U-235 fuel. Numbers in parenthesis are for Pu-239 fuel with similar flow rates and geometry.

TABLE VII

COMPARISON OF THE PERFORMANCE OF THE
IN-REACTOR TEST UNIT AND THE 1.2-MEGW R-F HEATER

	In-Reactor Test Unit	1.2-megw R-F Heater (FY 1970 Tests)*
Cavity inside diameter, in.	3.15	2.24
Cavity length, in.	8.4	2.0
Radiant heat flux per unit area, Btu/sec-ft^2	1130	6660
Equivalent black-body radiating temperature, deg R	7040	10,860
Operating pressure, atm	500	1-20
Buffer gas	Argon	Argon
Buffer injection velocity, ft/sec	9.6	10-50
Buffer weight flow, lb/sec	0.064	0.01-0.04

*Data from tests of Ref. 13

FIG. 1

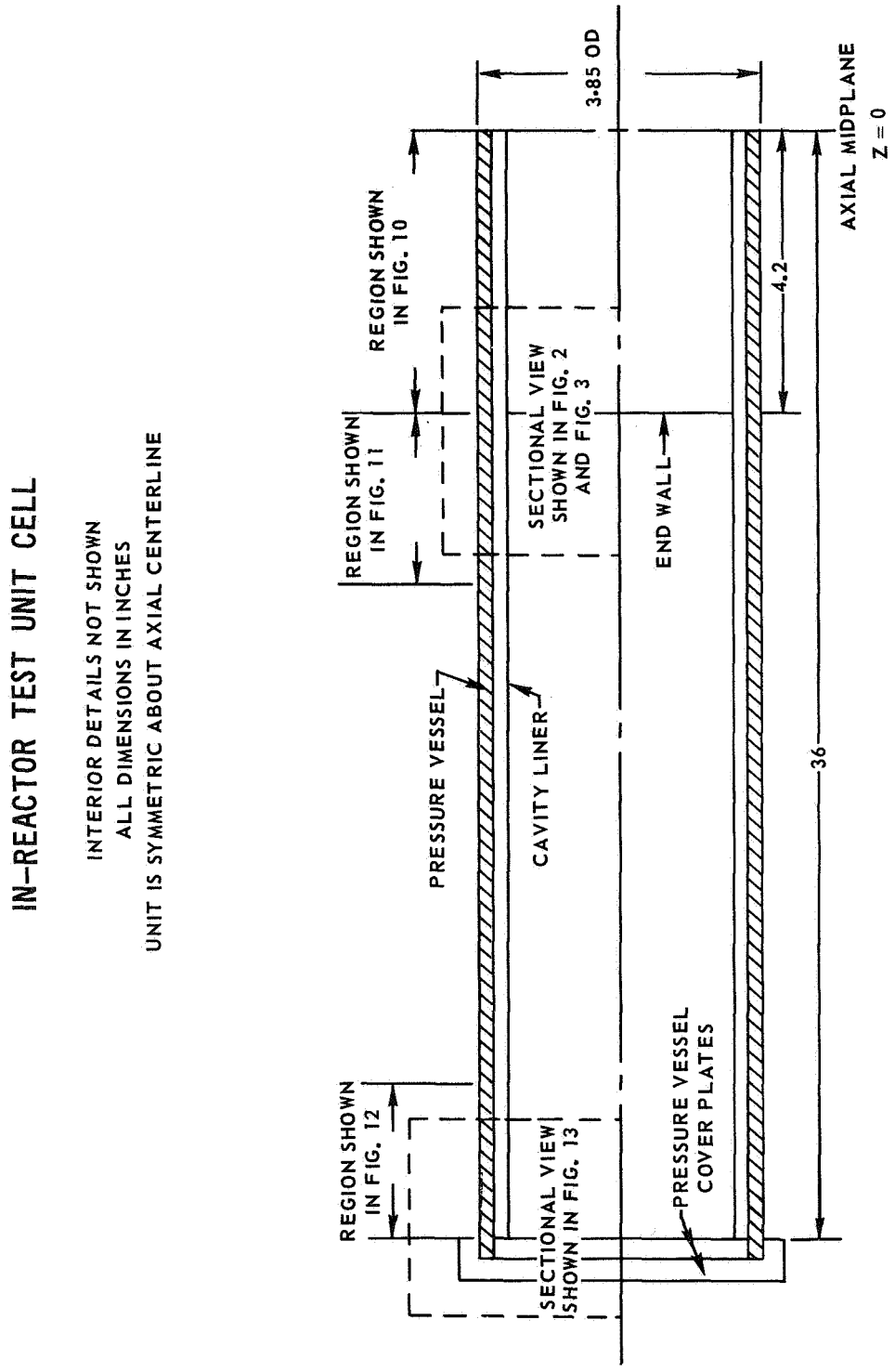
IN-REACTOR TEST UNIT CELL
INTERIOR DETAILS NOT SHOWN
ALL DIMENSIONS IN INCHES
UNIT IS SYMMETRIC ABOUT AXIAL CENTERLINE
REGION SHOWN IN FIG. 10
REGION SHOWN IN FIG. 11
REGION SHOWN IN FIG. 12
PRESSURE VESSEL
CAVITY LINER
SECTIONAL VIEW SHOWN IN FIG. 2 AND FIG. 3
SECTIONAL VIEW SHOWN IN FIG. 13
END WALL
PRESSURE VESSEL COVER PLATES
3.85 OD
4.2
36
AXIAL MIDPLANE
Z = 0

IN-REACTOR TEST UNIT CELL BASIC CONFIGURATIONS

TEST CELL LENGTH = 8.4 IN.

ALL DIMENSIONS IN INCHES

NUMBERS IN PARENTHESES DENOTE FLOW CIRCUITS DESCRIBED IN TEXT

SEE TABLES V AND VI FOR ADDITIONAL SPECIFICATIONS

(a) SECTION A-A

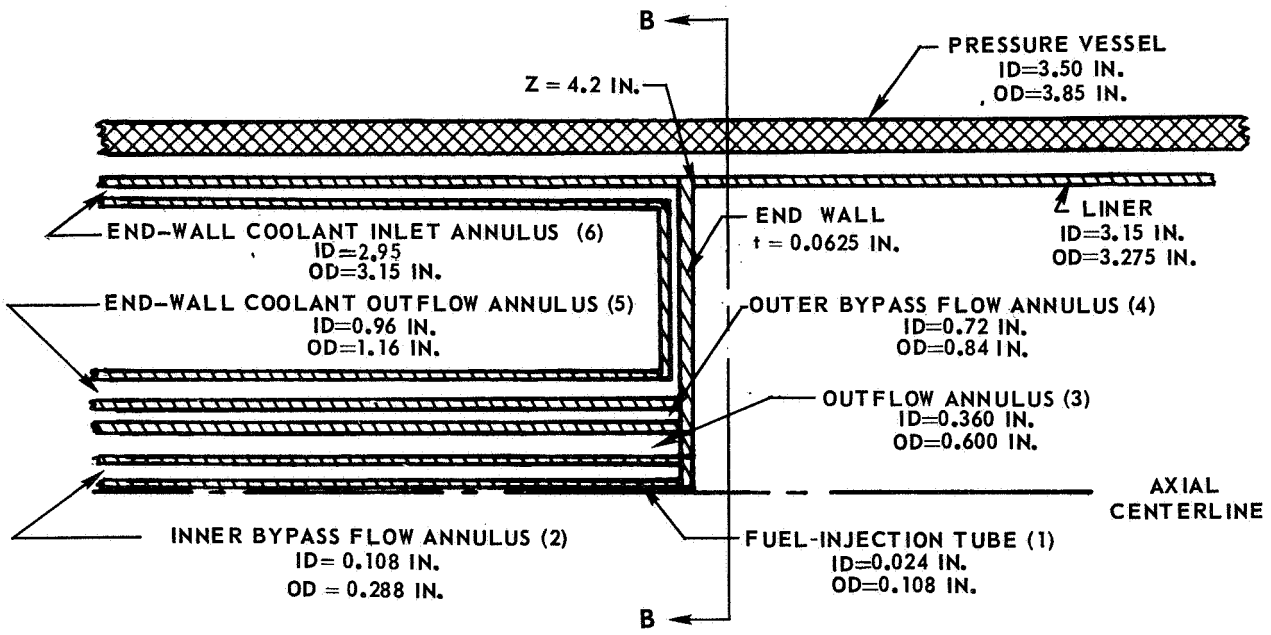

(b) SECTION B-B

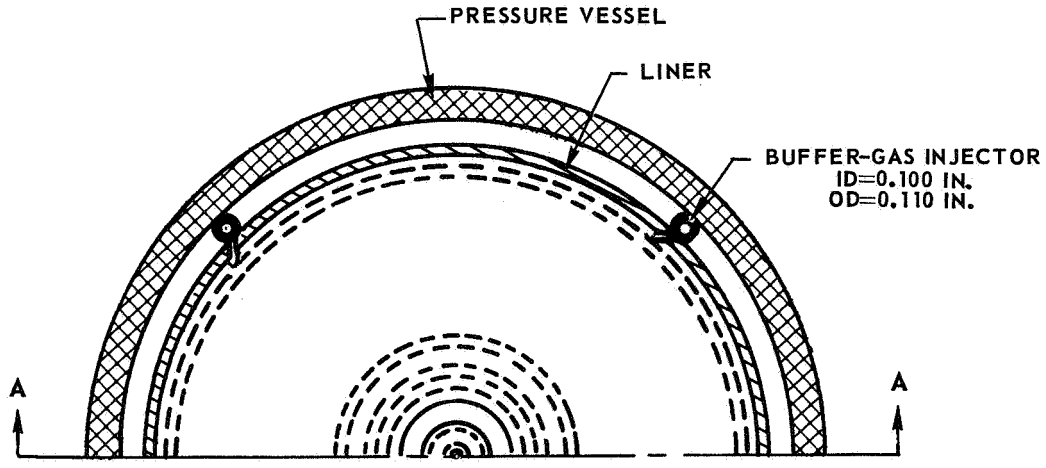

IN-REACTOR TEST UNIT CELL WITH OFF-CENTER FUEL INJECTION PORT

TEST CELL LENGTH 8.4 IN.
ALL DIMENSIONS IN INCHES

(a) SECTION A-A

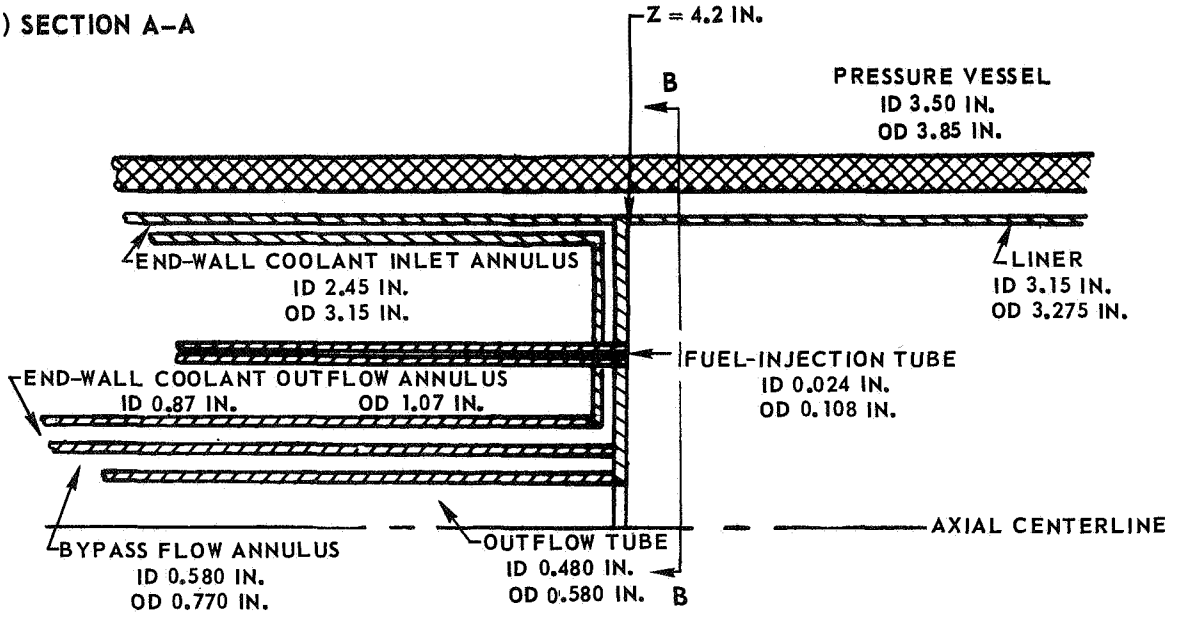

(b) SECTION B-B

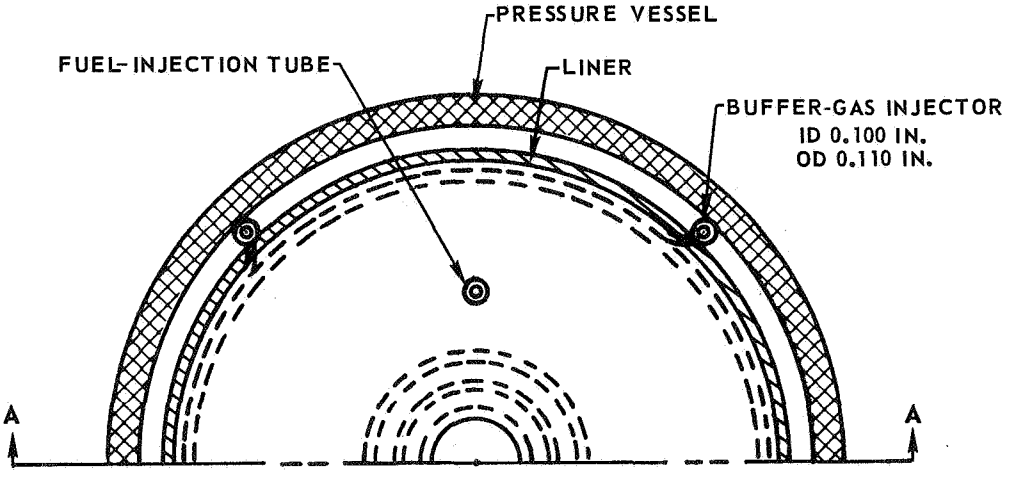

FIG. 4

IN-REACTOR TEST UNIT CELL FOR TESTS OF TRANSPARENT WALLS AND PROPELLANT HEATING

(a) TRANSPARENT-WALL TEST

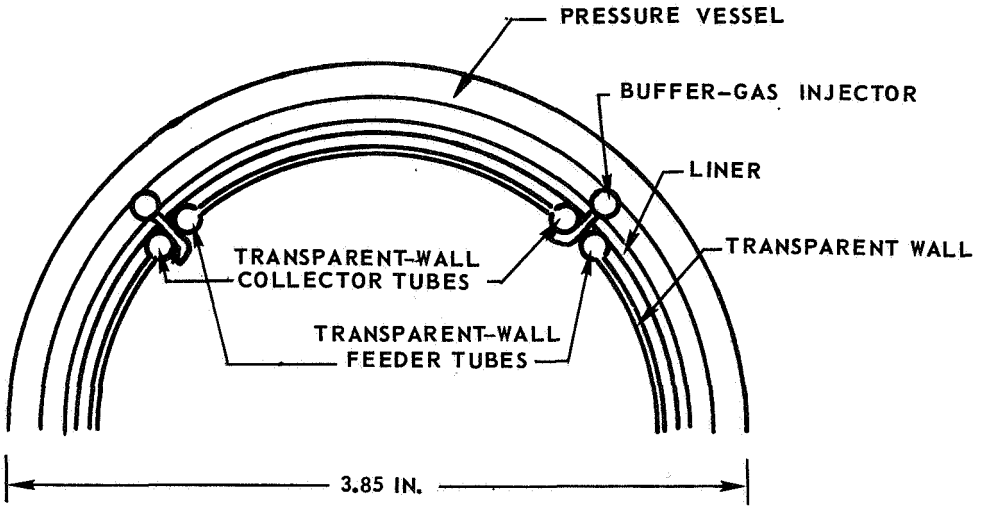

(b) TRANSPARENT-WALL AND PROPELLANT HEATING TEST

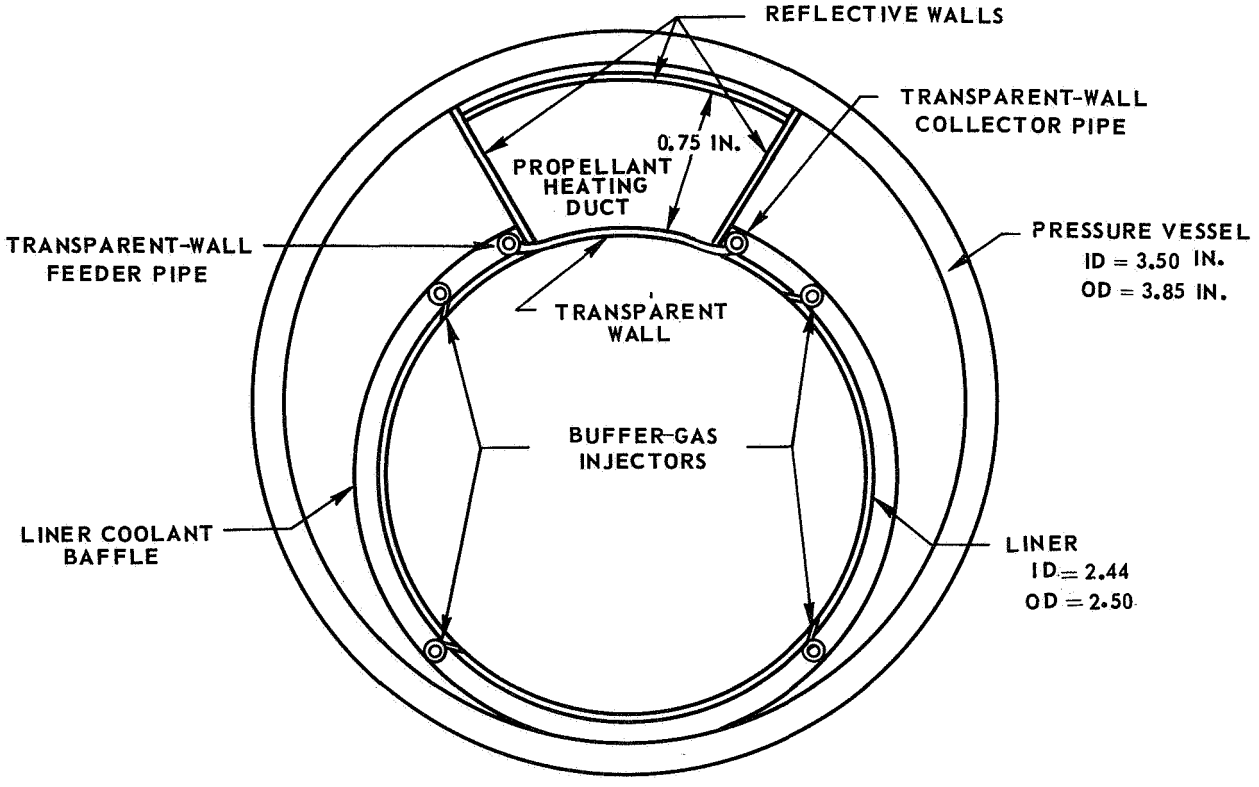

VARIATION OF AVERAGE FUEL PARTIAL PRESSURE WITH DENSITY FOR DIFFERENT VALUES OF RADIATIVE HEAT TRANSFER PER UNIT LENGTH

$\overline{P}_{F_6}$ = AVERAGE FUEL PRESSURE DUE TO NEUTRAL ATOMS, IONS, AND ELECTRONS BASED ON VOLUME WITHIN R_6

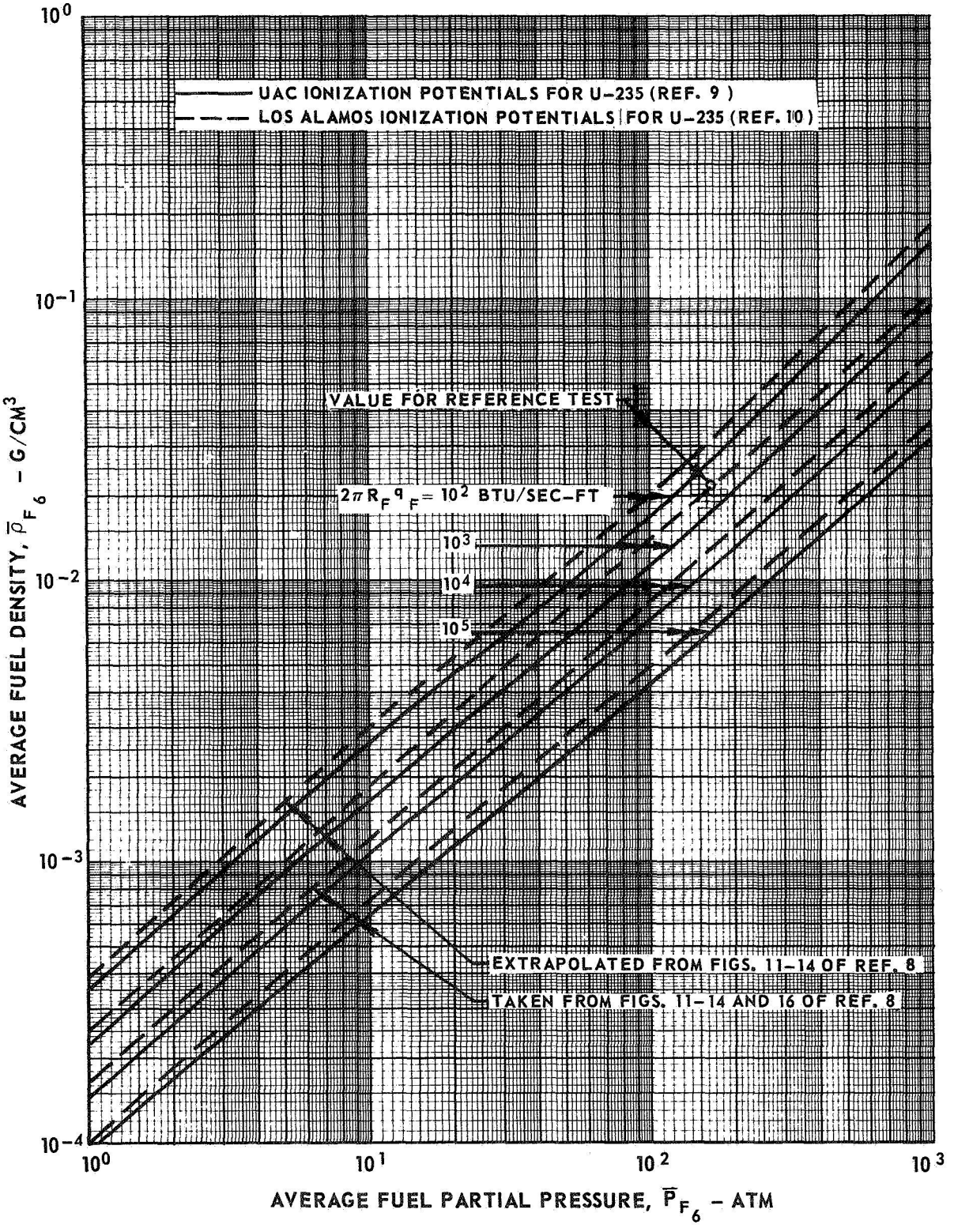

VARIATION OF RADIATING TEMPERATURES AND POWER LEVELS FOR NUCLEAR LIGHT BULB DEMONSTRATION TESTS

SPECIFICATIONS FOR UNIT CELL SHOWN IN FIGS. 1 AND 2

$R_T = 1.575$ IN. $R_F/R_T = 0.6$

$L_T = 8.40$ IN. $\overline{\rho}_{F_1}/\rho_{B_6} = 0.23$

$\mathcal{R} = 0.9$ $P_T = 500$ ATM

T^* ———————

Q_R — — — — — — — —

O DENOTES $\overline{P}_{F_6}$ FOR REFERENCE DESIGN

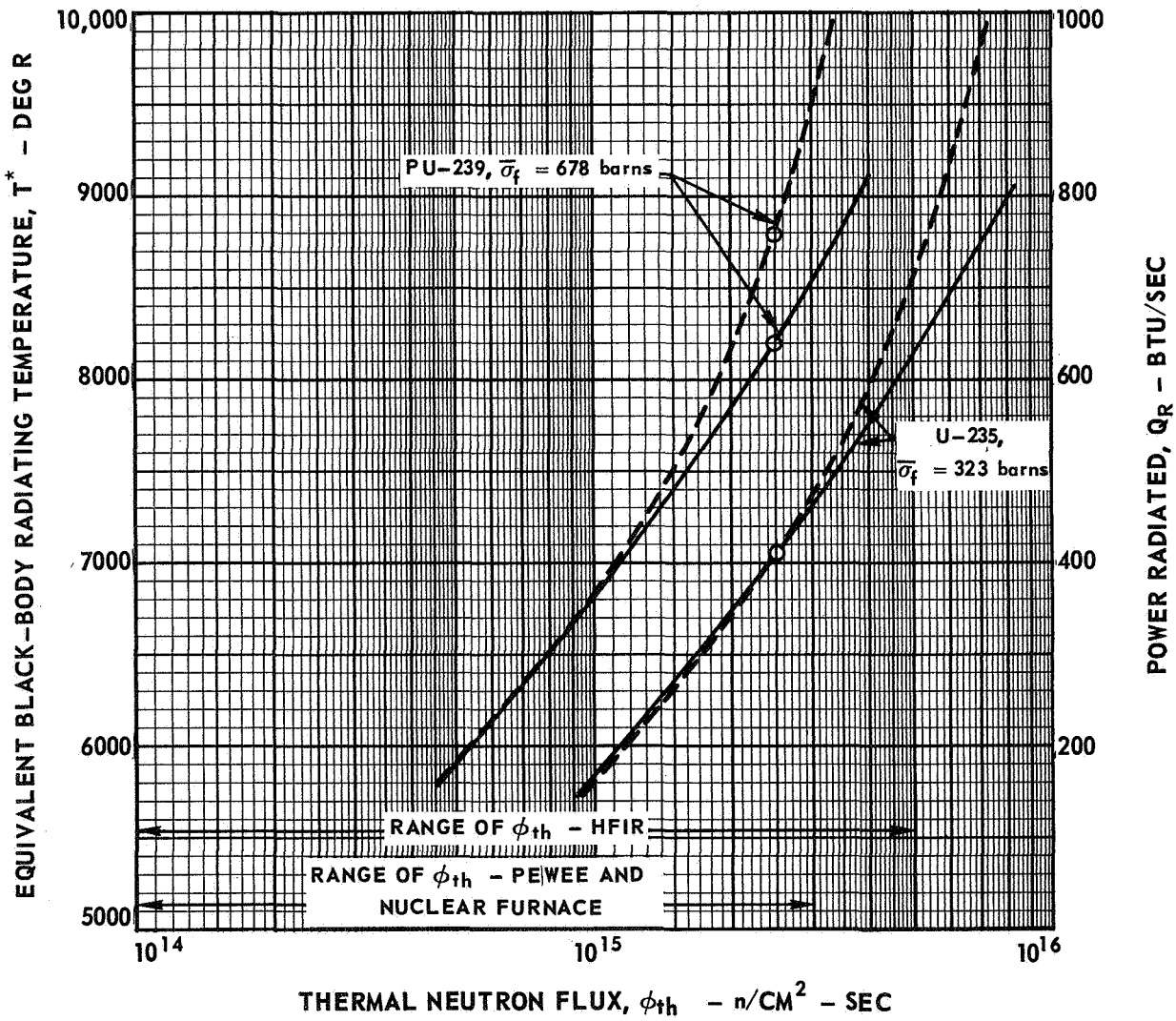

RANGES OF RADIATING TEMPERATURES AND POWER LEVELS

OPERATING PRESSURE, $P_T = 500$ ATM

THERMAL NEUTRON FLUX, $\phi_{th} = 2.5 \times 10^{15}$ n/CM^2-SEC

SPECIFICATIONS FOR UNIT CELL SHOWN IN FIGS. 1 AND 2

$R_T = 1.575$ IN. $\mathcal{R} = 0.9$

$R_F/R_T = 0.6$ $\bar{\rho}_{F_1}/\rho_{B_6} = 0.23$

$L_T = 8.40$ IN.

- - - - - - Pu - 239 ($\bar{\sigma}_f = 678$ b)

——— U - 235 ($\bar{\sigma}_f = 323$ b)

○ DENOTES $\bar{P}_{F_6}$ FOR REFERENCE DESIGN

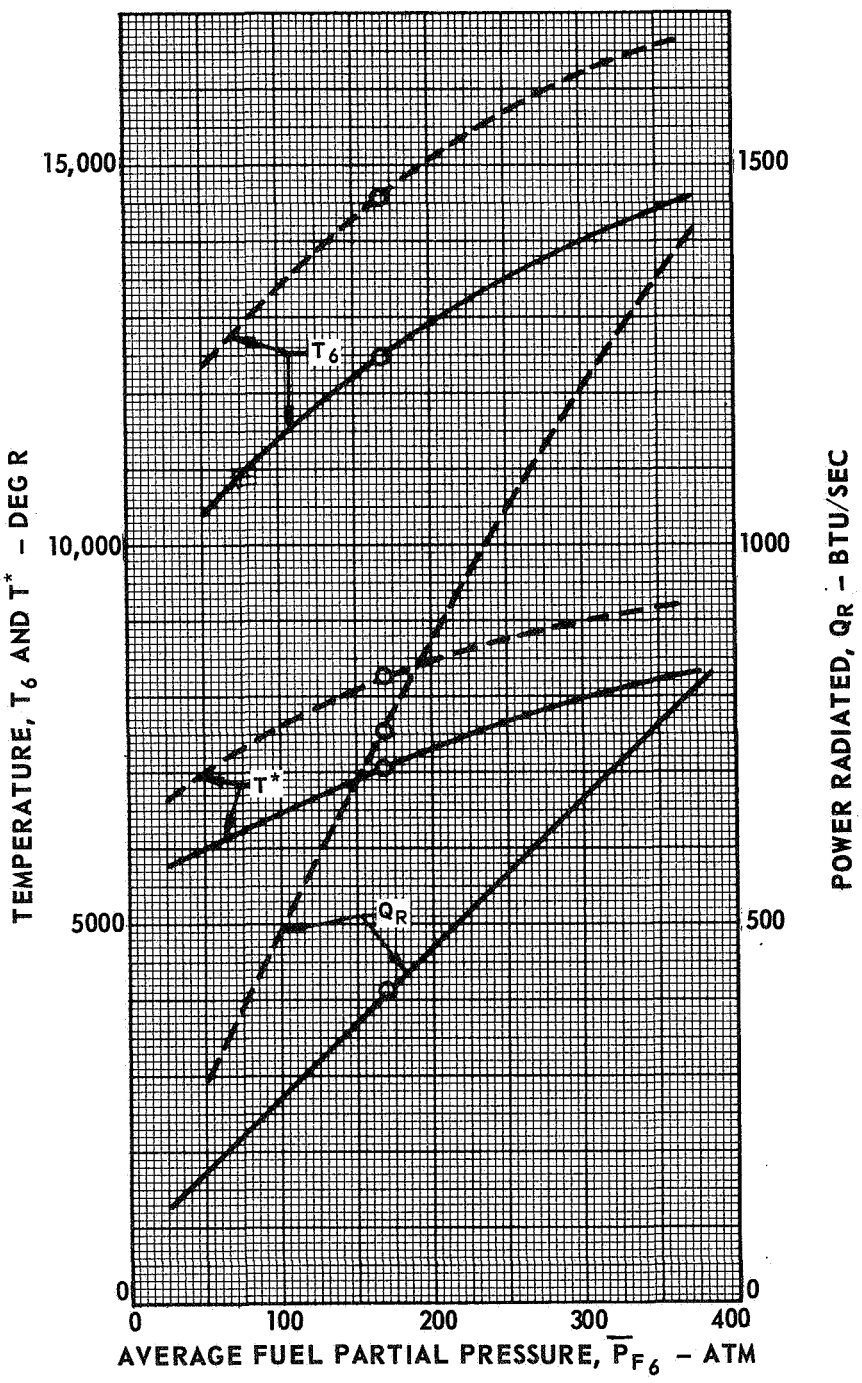

EFFECT OF VARIATIONS OF PARAMETERS AFFECTING IN-REACTOR TEST PERFORMANCE

ALL PARAMETERS HELD AT REFERENCE DESIGN VALUES EXCEPT FOR INDICATED VARIABLE

VALUES OF REFERENCE DESIGN PARAMETERS

$P_T = 500$ ATM	$\mathcal{R} = 0.9$
$R_T = 1.575$ IN.	$\bar{\rho}_{F_1}/\rho_{B_6} = 0.23$
$L_T = 8.40$ IN.	$R_F/R_T = 0.6$
$L_T/R_T = 5.33$	$\bar{\sigma}_f = 323$ b

$\phi_{th} = 2.5 \times 10^{15}$ n/CM^2 – SEC

O DENOTES REFERENCE DESIGN VALUES

(a) EFFECT OF VARIATION IN TEST REGION DIAMETER

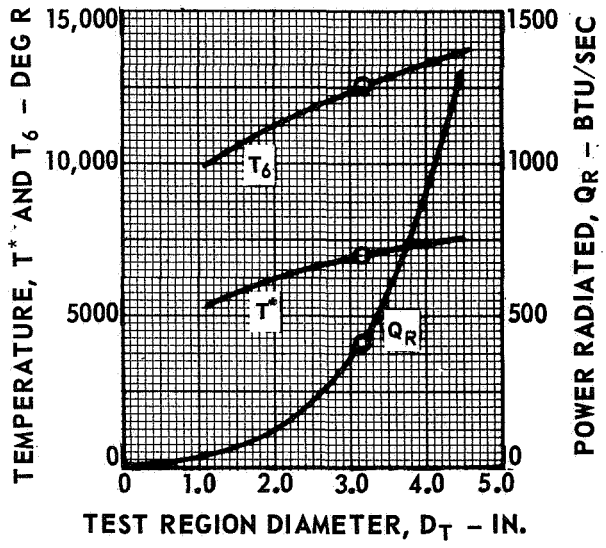

(b) EFFECT OF VARIATION IN DENSITY CONTAINMENT FACTOR

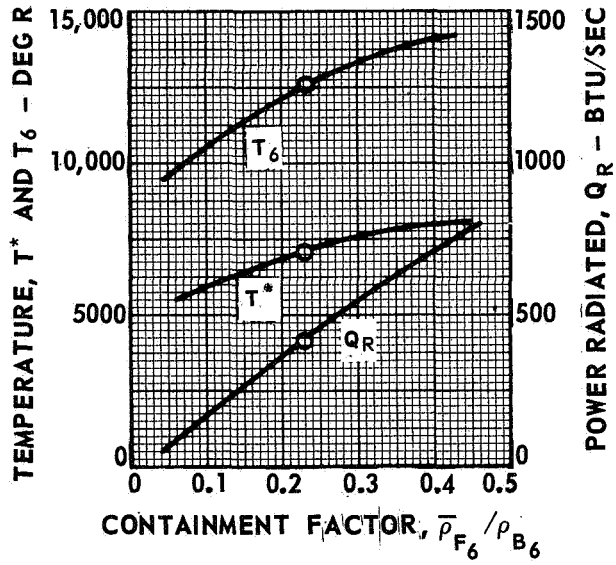

(c) EFFECT OF VARIATION IN ALUMINUM LINER REFLECTIVITY

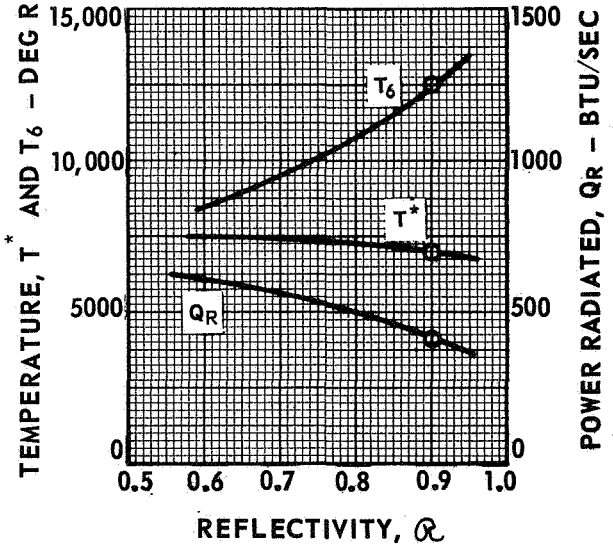

(d) EFFECT OF VARIATION IN FUEL-TO-CAVITY RADIUS RATIO

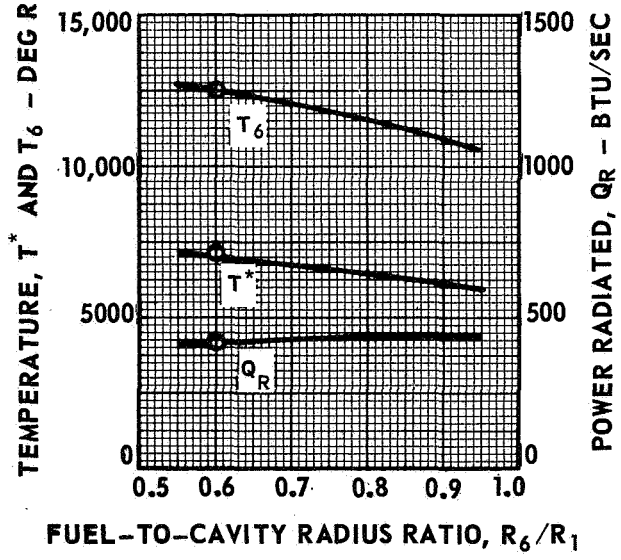

IN – REACTOR TEST UNIT CELL FLOW DIAGRAM

NUMBERS IN PARENTHESES DENOTE FLOW CIRCUITS DESCRIBED IN TEXT
SEE TABLES V AND VI FOR ADDITIONAL SPECIFICATIONS

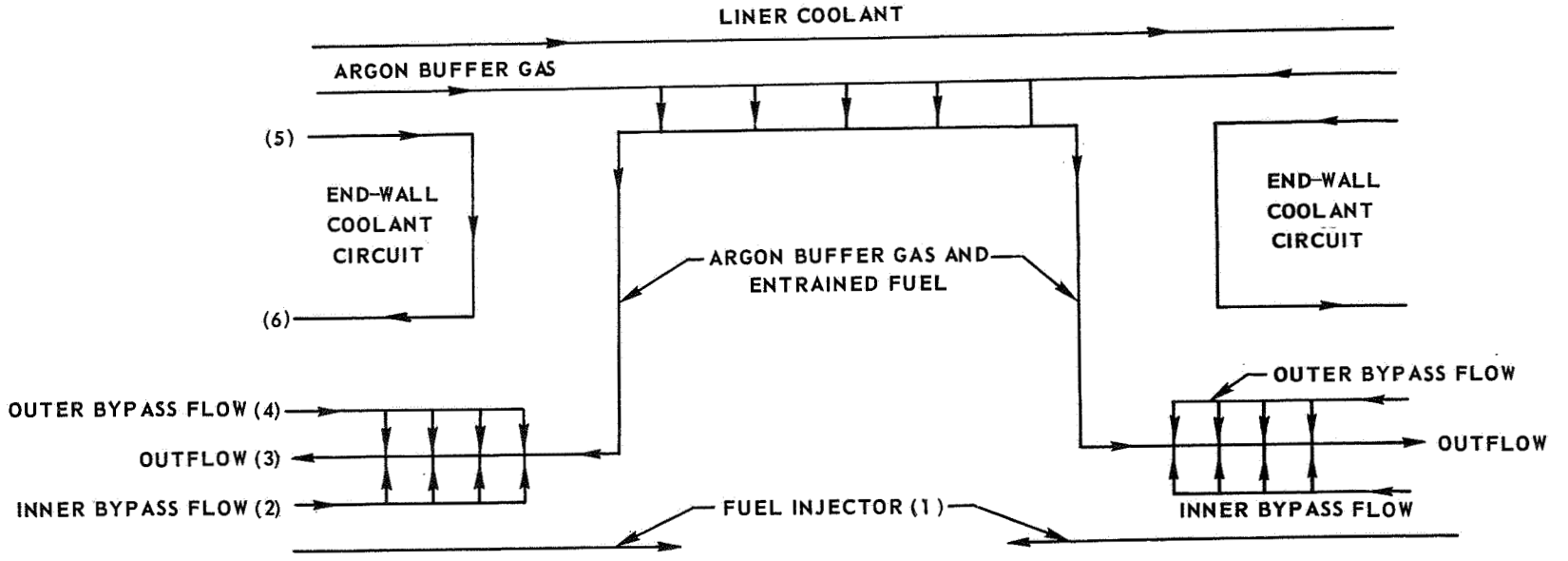

FIG. 9

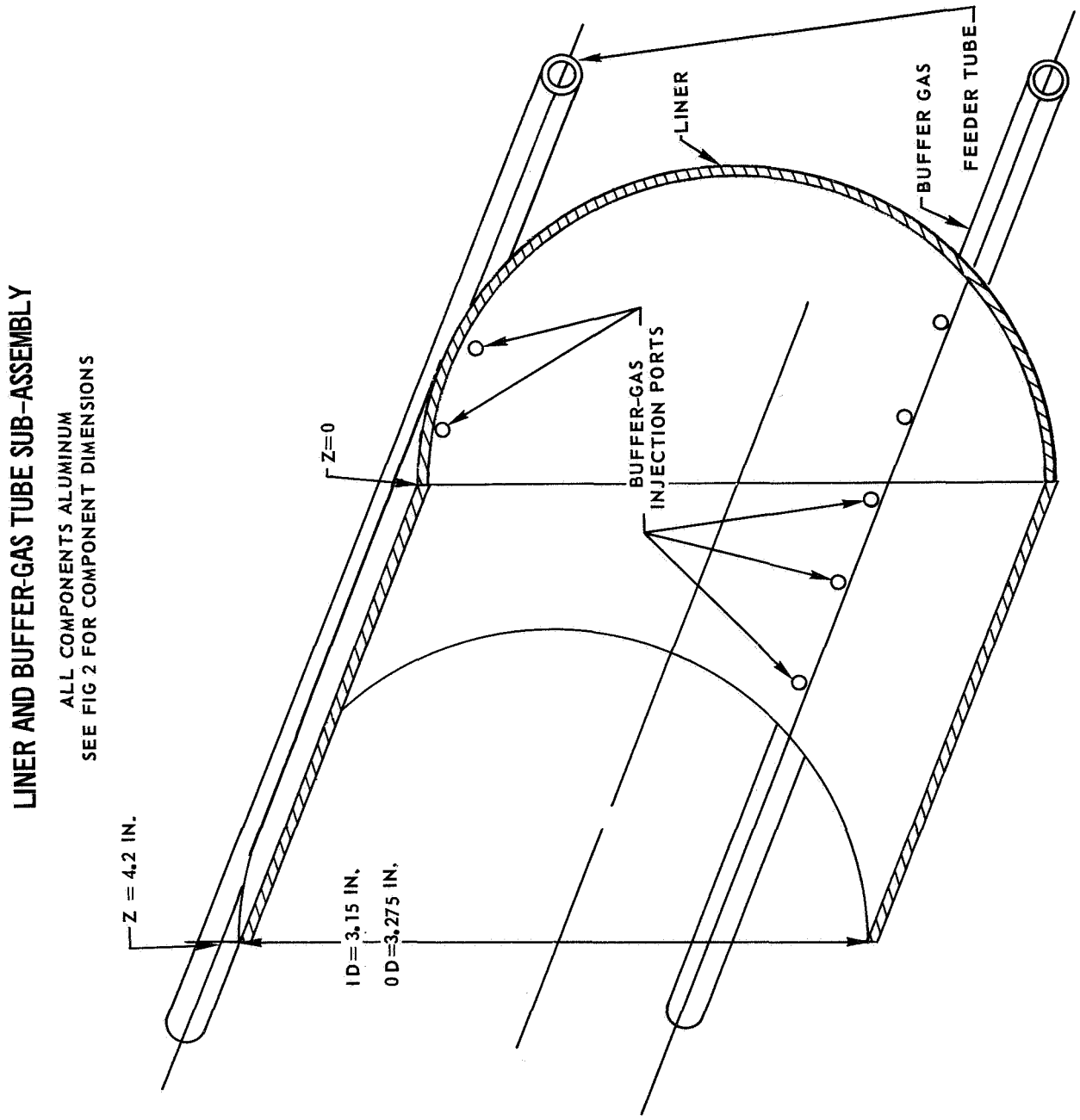
LINER AND BUFFER-GAS TUBE SUB-ASSEMBLY
ALL COMPONENTS ALUMINUM
SEE FIG 2 FOR COMPONENT DIMENSIONS
Z = 4.2 IN.
ID=3.15 IN.
OD=3.275 IN.
Z=0
BUFFER-GAS
INJECTION PORTS
LINER
BUFFER GAS
FEEDER TUBE

FIG. 11

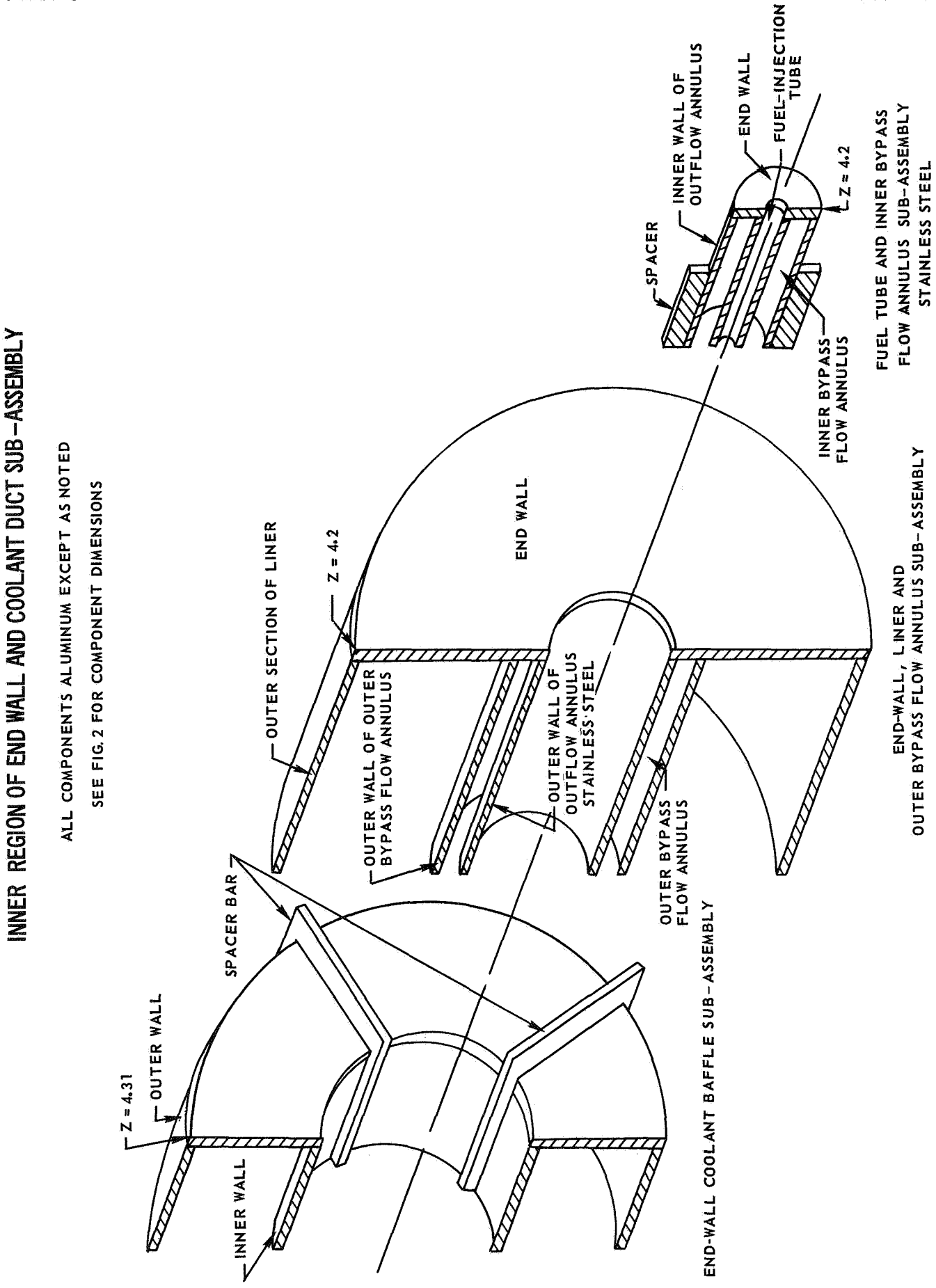
INNER REGION OF END WALL AND COOLANT DUCT SUB-ASSEMBLY
ALL COMPONENTS ALUMINUM EXCEPT AS NOTED
SEE FIG. 2 FOR COMPONENT DIMENSIONS
Z = 4.31
OUTER WALL
INNER WALL
SPACER BAR
END-WALL COOLANT BAFFLE SUB-ASSEMBLY
OUTER SECTION OF LINER
Z = 4.2
OUTER WALL OF OUTER BYPASS FLOW ANNULUS
END WALL
OUTER WALL OF OUTFLOW ANNULUS STAINLESS STEEL
OUTER BYPASS FLOW ANNULUS
END-WALL, LINER AND OUTER BYPASS FLOW ANNULUS SUB-ASSEMBLY
SPACER
INNER WALL OF OUTFLOW ANNULUS
END WALL
FUEL-INJECTION TUBE
Z = 4.2
INNER BYPASS FLOW ANNULUS
FUEL TUBE AND INNER BYPASS FLOW ANNULUS SUB-ASSEMBLY STAINLESS STEEL

OUTER REGION OF END WALL AND COOLANT DUCT SUB-ASSEMBLY

ALL COMPONENTS ALUMINUM EXCEPT AS NOTED
SEE FIG. 2 FOR COMPONENT DIMENSIONS

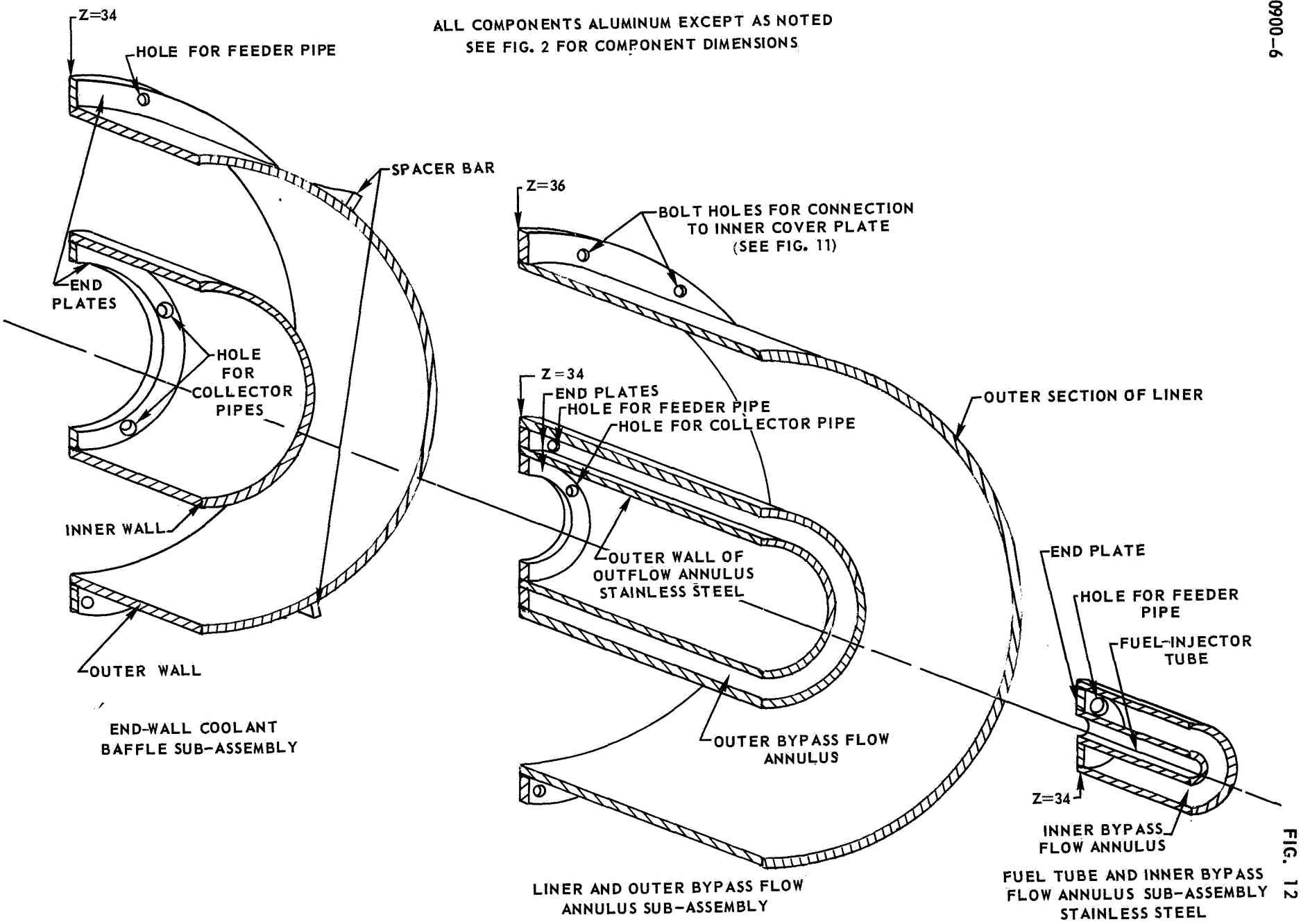

FIG. 12

SKETCH OF END WALL REGION OF IN-REACTOR TEST UNIT CELL

SEE FIG. 2 FOR COMPONENT DIMENSIONS

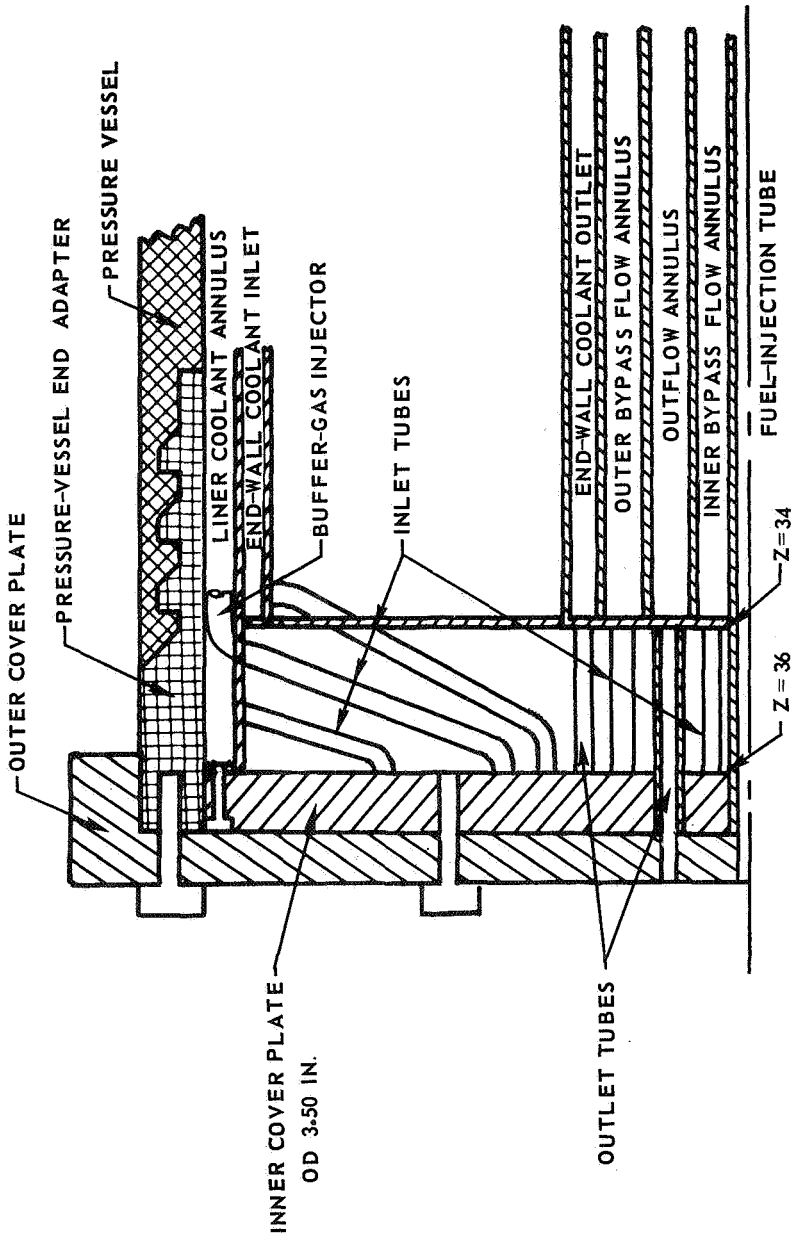

DISTRIBUTION LIST

NASA/AEC	Copy No.
Mr. Milton Klein Space Nuclear Propulsion Office U. S. Atomic Energy Commission Washington, D. C. 20545	1
Mr. F. C. Schwenk Space Nuclear Propulsion Office U. S. Atomic Energy Commission Washington, D. C. 20545	2
Captain C. E. Franklin Space Nuclear Propulsion Office U. S. Atomic Energy Commission Washington, D. C. 20545	3
Mr. R. F. Dickson Director of Technical Division Space Nuclear Propulsion Office c/o Nevada Operations Office U. S. Atomic Energy Commission Las Vegas, Nevada	4
U. S. Atomic Energy Commission Headquarters Library, Reports Section Mail Station G-017 Washington, D. C. 20545	5
Atomic Energy Commission Division of Technical Information Extension P. O. Box 62 Oak Ridge, Tennessee	6
Mr. John Marchaterre Argonne National Laboratory 9700 South Cass Avenue Argonne, Illinois	7

	Copy No.
Mr. L. P. Hatch Brookhaven National Laboratory Upton, Long Island, New York 11101	8
Los Alamos Scientific Laboratory P. O. Box 1663 Los Alamos, New Mexico 87544 Attention: N Division	9
Mr. Keith Boyer N Division Los Alamos Scientific Laboratory Los Alamos, New Mexico 87544	10
Mr. T. R. Cotter Los Alamos Scientific Laboratory Los Alamos, New Mexico 87544	11
Dr. R. D. Cowan Los Alamos Scientific Laboratory Los Alamos, New Mexico 87544	12
Dr. George Grover N-5 Los Alamos Scientific Laboratory P. O. Box 1663 Los Alamos, New Mexico 87544	13
Dr. William Kirk Los Alamos Scientific Laboratory P. O. Box 1663 Los Alamos, New Mexico 87544	14
Mr. John D. Orndoff N Division Los Alamos Scientific Laboratory Los Alamos, New Mexico 87544	15
Dr. L. J. Radziemski Los Alamos Scientific Laboratory Los Alamos, New Mexico 87544	16

	Copy No.
Dr. D. W. Steinhaus Los Alamos Scientific Laboratory Los Alamos, New Mexico 87544	17
Dr. T. F. Stratton Los Alamos Scientific Laboratory Los Alamos, New Mexico 87544	18
Mr. E. A. Franco-Ferreira Metals & Ceramics Division Oak Ridge National Laboratory P. O. Box X Oak Ridge, Tennessee 37831	19
Mr. A. P. Fraas Oak Ridge National Laboratory P. O. Box Y Oak Ridge, Tennessee 37831	20
Dr. John J. Keyes, Jr. Reactor Division Oak Ridge National Laboratory P. O. Box Y Oak Ridge, Tennessee 37831	21
Mr. P. Patriarca Oak Ridge National Laboratory P. O. Box X Oak Ridge, Tennessee 37831	22
NASA Headquarters Washington, D. C. 20546 Attention: New Technology Representative, Code UT	23
NASA Headquarters Washington, D. C. 20546 Attention: OART	24
National Aeronautics and Space Administration Office of Scientific and Technical Information Washington, D. C. 20546 Attention: AFSS-LL	25

	Copy No.
National Aeronautics and Space Administration Washington, D. C. 20546 Attention: Office of Technical Information and Educational Programs, Code ETL	26
NASA Scientific and Technical Information Facility (2 copies) Post Office Box 33 College Park, Maryland 20740	27 28
Dr. A. J. Eggers, Jr. Office of Advanced Research and Technology NASA Headquarters 1520 H Street, NW Washington, D. C. 20546	29
Mr. A. E. Gessow NASA Headquarters Office of Advanced Research and Technology Washington, D. C. 20546	30
Dr. K. Thom Code RRE NASA Headquarters Washington, D. C. 20546	31
Mr. R. W. Ziem (RPS) National Aeronautics and Space Administration Washington, D. C. 20546	32
Mr. H. Hornby NASA Ames Research Center Mission Analysis Division Moffett Field, California 94035	33
Dr. W. L. Love NASA-Ames Research Center Magnetoplasmadynamics Branch Mail Stop N-229-2 Moffett Field, California 94035	34

	Copy No.
Dr. Chul Park NASA-Ames Research Center Magnetoplasmadynamics Branch Mail Stop N-299-2 Moffett Field, California 94035	35
Mr. C. A. Syvertson Associate Director for Astronautics NASA-Ames Research Center Moffett Field, California 94035	36
NASA Goddard Space Flight Center Glenn Dale Road Greenbelt, Maryland Attention: Librarian	37
Jet Propulsion Laboratory/CAL TECH 4800 Oak Grove Drive Pasadena, California 91103 Attention: Library Section 111-113	38
Mr. D. R. Bartz Manager, Research and Advanced Concepts Section Propulsion Division Jet Propulsion Laboratory Pasadena, California 91103	39
Mr. Jerry P. Davis Building 122-3 Jet Propulsion Laboratory 4800 Oak Grove Drive Pasadena, California 91103	40
Dr. Clifford J. Heindl Building 180-805 Jet Propulsion Laboratory 4800 Oak Grove Drive Pasadena, California 91103	41
Dr. Robert V. Meghreblian Jet Propulsion Laboratory 4800 Oak Grove Avenue Pasadena, California 91103	42

	Copy No.
Mr. L. E. Newlan Chief, Reports Groups Jet Propulsion Laboratory 4800 Oak Grove Drive Pasadena, California 91103	43
Mr. Gary R. Russell Jet Propulsion Laboratory California Institute of Technology 4800 Oak Grove Drive Pasadena, California 91103	44
National Aeronautics and Space Administration Langley Research Center Langley Air Force Base Virginia Attention: Library	45
Dr. F. Allario National Aeronautics & Space Administration Langley Research Center Langley Station Hampton, Virginia 23365	46
Dr. R. V. Hess National Aeronautics & Space Administration Langley Research Center Langley Station Hampton, Virginia 23365	47
Mr. R. A. Lucht National Aeronautics & Space Administration Langley Research Center Langley Station Hampton, Virginia 23365	48
Major R. C. Chaplin, AFSC/STLO NASA-Lewis Research Center 21000 Brookpark Road Cleveland, Ohio 44135	49

	Copy No.
Dr. J. C. Evvard Associate Director Mail Stop 3-5 NASA-Lewis Research Center 21000 Brookpark Road Cleveland, Ohio 44135	50
Dr. Richard W. Patch Nuclear Systems Division Mail Stop 106-1 NASA-Lewis Research Center 21000 Brookpark Road Cleveland, Ohio 44135	51
Mr. Robert G. Ragsdale Nuclear Systems Division Mail Stop 106-1 NASA-Lewis Research Center 21000 Brookpark Road Cleveland, Ohio 44135	52
Mr. Frank E. Rom Nuclear Systems Division Mail Stop 106-1 NASA-Lewis Research Center 21000 Brookpark Road Cleveland, Ohio 44135	53
National Aeronautics and Space Administration Manned Spacecraft Center P. O. Box 1537 Houston, Texas Attention: Library	54
National Aeronautics and Space Administration George C. Marshall Space Flight Center Huntsville, Alabama 35812 Attention: Library	55
Mr. Ronald J. Harris Chief, Planetary & Nuclear Systems Group Advanced Systems Office R-AS George C. Marshall Space Flight Center Huntsville, Alabama 35812	56

DOD	Copy No.
Dr. U. Bauder Thermomechanics Research Lab Department of the Air Force Aerospace Research Lab (OAR) Wright-Patterson AFB, Ohio 45433	57
Col. W. Jakomis Department of the Air Force Aerospace Research Lab (OAR) Wright-Patterson AFB, Ohio 45433	58
Dr. H. Schrade Thermomechanics Research Lab Department of the Air Force Aerospace Research Lab (OAR) Wright-Patterson AFB, Ohio 45433	59
Mr. Erich E. Soehngen, Director Thermomechanics Research Lab Code ARN Aerospace Research Lab Wright-Patterson AFB, Ohio 45433	60
Lt. B. Turman Thermomechanics Research Lab Department of the Air Force Aerospace Research Lab (OAR) Wright-Patterson AFB, Ohio 45433	61
Dr. Hans von Ohain Aerospace Research Lab (ARD-1) Wright-Patterson AFB, Ohio 45433	62
Mr. E. C. Perkins AUL (AUL3T-7143) Maxwell Air Force Base Alabama	63
Dr. Charles J. Bridgman Associate Professor of Physics Air Force Institute of Technology Wright-Patterson AFB, Ohio 45433	64

	Copy No.
Captain E. N. Kemler Office of Research Analysis Holloman Air Force Base New Mexico	65
Dr. J. F. Masi (SREP) Department of the Air Force Air Force Office of Scientific Research 1400 Wilson Boulevard Arlington, Virginia 22209	66
Mr. L. J. Edwards Air Force Rocket Propulsion Laboratory Edwards AFB, California 93523	67
Mr. G. Sayles (RPRRA) Air Force Rocket Propulsion Laboratory Edwards AFB, California 93523	68
HQ-SAMSO (SMAAP/Capt. Yepp) Air Force Unit Post Office Los Angeles Air Force Station California 90045	69
AFSC (SCTD) Andrews Air Force Base Washington, D. C.	70
Commander AFSC Foreign Technology Division Wright-Patterson AFB, Ohio 45433 Attention: RTD (TD-E3b)	71
Aerospace Corporation P. O. Box 95085 Los Angeles, California 90045 Attention: Library-Documents	72
Dr. Robert F. Trapp Chief, Research Division Weapons Evaluation and Control Bureau Arms Control and Disarmament Agency 320 21st Street, NW Washington, D. C. 20451	73

	Copy No.
Mr. J. E. Jackson DDR&E (OAP) Washington, D. C.	74
DDR&E (WSEG) Washington, D. C. Attention: OSD	75
Dr. Theodore B. Taylor Defense Atomic Support Agency The Pentagon Washington, D. C. 20301	76
Lt. N. Kuehn Defense Intelligence Agency The Pentagon, Attn: DIA ST-2C2 Washington, D. C. 20301	77
Dr. Robert H. Fox Institute for Defense Analysis 400 Army Navy Drive Arlington, Virginia 22202	78
Dr. W. N. Podney Institute for Defense Analysis 400 Army Navy Drive Arlington, Virginia 22202	79
Superintendent U. S. Naval Postgraduate Naval Academy Monterey, California	80
Mr. George T. Lalos U. S. Naval Ordnance Laboratory White Oaks, Silver Springs Maryland 20900	81
Naval Plant Representative Office c/o UAC Pratt & Whitney Aircraft Division East Hartford, Connecticut 06108 Attention: Mr. R. F. Parslow	82

	Copy No.
The Rand Corporation 1700 Main Street Santa Monica, California 90406	83
Mr. E. C. Gritton The Rand Corporation 1700 Main Street Santa Monica, California 90406	84
Mr. Ben Pinkel The Rand Corporation 1700 Main Street Santa Monica, California 90406	85

OTHERS

Dr. J. W. Hilborn Reactor Physics Branch Advanced Projects & Reactor Physics Division Atomic Energy of Canada Limited Chalk River, Ontario, Canada	86
National Aeronautics and Space Council Attention: W. E. Berg Executive Office of the President Washington, D. C. 20502	87
Dr. Charles Beckett Heat Division National Bureau of Standards Washington, D. C.	88
Mr. Frederick C. Durant, III Assistant Director, Astronautics National Air Museum Smithsonian Institute Washington, D. C. 20560	89

INDUSTRY	Copy No.
Aerojet-General Corporation P. O. Box 1947 Sacramento, California 95809 Attention: Technical Information Office	90
Mr. William J. Houghton Department 7830, Building 2019A2 Aerojet-General Corporation P. O. Box 15847 Sacramento, California 95813	91
Mr. Joseph J. Peterson Aerojet-General Corporation Department 700, Building 2019A2 P. O. Box 15847 Sacramento, California 95813	92
B. Probert Aerojet-General Nucleonics P. O. Box 78 San Ramon, California	93
Mr. W. L. Snapp Aerojet-General Corporation 20545 Center Ridge Road Cleveland, Ohio 44116	94
Dr. J. J. Stewart Department 7040, Building 2019A2 Aerojet-General Corporation Sacramento, California 95813	95
Florence Walsh, Librarian Aerojet-General Corporation 11711 South Woodruff Avenue Downey, California	96
Mr. D. F. Vanica Aerojet Nuclear Systems Company Department 7020, Building 2019A2 P. O. Box 15847 Sacramento, California 95813	97

	Copy No.
Mr. Michael J. Monsler AVCO-Everett Research Laboratory 2385 Revere Beach Parkway Everett, Massachusetts 02149	98
Dr. Richard Rosa AVCO-Everett Research Laboratory 2385 Revere Beach Parkway Everett, Massachusetts 02149	99
Mr. Jerrold M. Yos AVCO Corporation Research & Advanced Development Division 201 Lowell Street Wilmington, Massachusetts 01887	100
Bell Aerosystems Box 1 Buffalo, New York Attention: T. Reinhardt	101
Mr. R. R. Barber Boeing Company Aerospace Division P. O. Box 3707 Seattle, Washington 98124	102
Mr. J. A. Brousseau Chief, Propulsion Systems Technology Mail Stop 47-18 The Boeing Company Seattle, Washington 98124	103
Mr. Richard W. Carkeek The Boeing Company P. O. Box 3868 Mail Stop 85-85 Seattle, Washington 98124	104
Dr. Jacob B. Romero The Boeing Company Mail Stop 84-66 Kent, Washington	105

	Copy No.
Crysler Corporation Defense Operations Division Box 757 Detroit 31, Michigan	106
Mr. Arthur Sherman Computer & Applied Sciences, Inc. 9425 Stenton Avenue Philadelphia, Pennsylvania 19118	107
Dr. Robert W. Bussard Corporation Chief Scientist CSI Corporation 1801 Avenue of the Stars Suite 934 Los Angeles, California 90067	108
Dr. Ralph S. Cooper Donald W. Douglas Laboratories 2955 George Washington Way Richland, Washington 99352	109
Dr. D. E. Knapp Donald W. Douglas Laboratories 2955 George Washington Way Richland, Washington 99352	110
Dr. R. J. Holl Missiles & Space Systems Division Douglas Aircraft Company Santa Monica, California 90405	111
Dr. Kurt P. Johnson Advanced Space Technology, A2-263 Douglas Missiles & Space Systems Division Santa Monica, California 90405	112
Mr. J. L. Waisman Douglas Aircraft Company Santa Monica, California 90405	113

	Copy No.
General Atomics Division General Dynamics Corporation P. O. Box 1111 San Diego, California 92112	114
Dr. J. R. Beyster General Atomics Division General Dynamics Corporation P. O. Box 608 San Diego, California 92112	115
Mr. Louis Canter General Dynamics/Astronautics Technical Library San Diego, California 92112	116
Mr. James Nance General Atomics Division General Dynamics Corporation P. O. Box 608 San Diego, California 92112	117
Mr. John Peak General Atomics Division General Dynamics Corporation P. O. Box 608 San Diego, California 92112	118
Dr. John Romanko, Staff Scientist Y-128, Building 197 General Dynamics Ft. Worth Division, Box 740 Ft. Worth, Texas 76101	119
General Electric Company MSVD Library Documents Group, RM 3446 3198 Chestnut Street Philadelphia, Pennsylvania 19101	120
General Electric Company Cincinnati, Ohio 45215 Attention: Technical Information Center	121

	Copy No.
Mr. Carmen B. Jones H63 - General Electric Company North I-75 Cincinnati, Ohio 45215	122
Dr. S. M. Scala Manager, Theoretical Fluid Physics Section General Electric Company Space Sciences Laboratory P. O. Box 8555 Philadelphia, Pennsylvania 19101	123
Mr. J. W. Stephenson General Electric Company, NMPO P. O. Box 15132 Cincinnati, Ohio 45215	124
R. R. Blackwell Allison Division General Motors Corporation P. O. Box 24013 Indianapolis, Indiana 46206	125
Mr. David Mallon Allison Division General Motors Corporation 2355 S. Tibbs Avenue Indianapolis, Indiana 46206	126
Dr. Jerry Grey Grey-Rad Corporation 12 Station Drive Princeton, New Jersey 08540	127
Mr. M. O. Friedlander Engineering Library, Plant 5 Grumman Aircraft Engineering Corporation Bethpage, Long Island, New York	128
Mr. Thomas N. Delmer Gulf General Atomic, Inc. P. O. Box 608 San Diego, California 92112	129

	Copy No.
Dr. J. F. Kunze, Manager Operations & Analysis Idaho Test Station Idaho Nuclear Corporation P. O. Box 1845 Idaho Falls, Idaho 83401	130
Dr. J. W. Morfitt, Manager Idaho Test Station Idaho Nuclear Corporation P. O. Box 1845 Idaho Falls, Idaho 83401	131
Isotopes Nuclear Systems Division 110 West Timonium Road Timonium, Maryland 21093 Attention: Library	132
Miss Belle Berlad, Librarian Lockheed Propulsion Company P. O. Box 111 Redland, California	133
Mr. Holmes F. Crouch Lockheed Missiles & Space Company Space System Division, Dept. 62-90, Building 104 Sunnyvale, California 94408	134
Mr. Maxwell Hunter Department 50-01, Building 102 Lockheed Missiles & Space Company P. O. Box 504 Sunnyvale, California 94408	135
Dr. Larry Kaufman Director of Research Manlabs, Inc. 21 Erie Street Cambridge, Massachusetts 02139	136

	Copy No.
Mr. J. J. Norton Marquardt Corporation 16555 Saticoy Street Van Nuys, California	137
Mr. W. H. Morita North American Aviation, Inc. Space & Information Systems Division 12214 Lakewood Boulevard Downey, California	138
North American Aviation, Inc. Space & Information Systems Division 12214 Lakewood Boulevard Downey, California Attention: Technical Information Center (L. M. Foster)	139
Professor Abraham Hyatt North American Rockwell Corporation Aerospace & Systems Group 1700 E. Imperial Highway El Segundo, California 90246	140
Dr. A. G. Randol III Nuclear Fuel Services Wheaton Plaza Building Wheaton, Maryland 20902	141
Rocketdyne 6633 Canoga Park, California 91303 Attention: Library, Dept. 596-306	142
Mr. C. C. Bennett Rocketdyne P. O. Box 552 Canoga Park, California 91303	143
Mr. Robert Dillaway Nucleonics Department Rocketdyne 6633 Canoga Avenue Canoga Park, California 91303	144

	Copy No.
Dr. S. V. Gunn Rocketdyne 6633 Canoga Avenue Canoga Park, California 91303	145
Space Technology Laboratories One Space Park Redondo Beach, California 90277 Attention: STL Technical Library Doc. Acquisitions	146
Mr. Merle Thorpe TAFA Division Humphreys Corporation 180 North Main Street Concord, New Hampshire 03301	147
Thompson Ramo Wooldridge 23555 Euclid Avenue Cleveland, Ohio Attention: Librarian	148
Mr. Walter F. Krieve Building S TRW Systems One Space Park Redondo Beach, California 90278	149
Dr. D. W. Drawbaugh Astronuclear Laboratory Westinghouse Electric Corporation Pittsburgh, Pennsylvania 15236	150
Mr. Jack Felchtner Westinghouse Research Labs Churchill Borough Pittsburgh, Pennsylvania 15285	151
Mr. M. R. Keller Westinghouse Electric Corporation Astronuclear Laboratory Pittsburgh, Pennsylvania 15200	152

	Copy No.
Mr. F. McKenna Astronuclear Laboratory Westinghouse Electric Corporation P. O. Box 10864 Pittsburgh, Pennsylvania 15236	153
Dr. Jack Ravets Westinghouse Astronuclear Laboratory P. O. Box 10864 Pittsburgh, Pennsylvania 15236	154
Dr. Henry Stumpf Astronuclear Laboratory Westinghouse Electric Corporation Pittsburgh, Pennsylvania 15236	155
Mr. Y. S. Tang Westinghouse Electric Corporation Astronuclear Laboratory Pittsburgh, Pennsylvania 15200	156
UNIVERSITIES	
Dr. John Hanlin College of Engineering Auburn University Auburn, Alabama 36833	157
Dr. Ken Pell College of Engineering Auburn University Auburn, Alabama 36833	158
Dr. C. C. Chang Head, Space Sciences & Applied Physics Catholic University of America Washington, D. C. 20017	159
Professor Robert A. Gross School of Engineering & Applied Science Columbia University New York, New York 10027	160

	Copy No.
Professor Chieh Ho Division of Nuclear Science Room 287, Mudd Building Columbia University New York, New York 10027	161
Professor Terence Cool Thermal Engineering Department Cornell University Ithaca, New York 14850	162
Dr. G. H. Miley Ward Reactor Laboratory Department of Applied Physics College of Engineering Cornell University Ithaca, New York 14850	163
Dr. Franklin K. Moore, Head Thermal Engineering Department Cornell University Ithaca, New York 14850	164
Mr. D. J. Strobel Department of Thermal Engineering Cornell University 208 Upson Hall Ithaca, New York 14850	165
Dr. Joseph Clement Nuclear Engineering Department Georgia Institute of Technology Atlanta, Georgia 30332	166
Dr. W. R. Jacobs School of Nuclear Engineering Georgia Institute of Technology Atlanta, Georgia 30332	167
Professor Clyde Orr, Jr. Chemical Engineering Department Georgia Institute of Technology Atlanta, Georgia 30332	168

	Copy No.
Dr. S. V. Shelton School of Nuclear Engineering Georgia Institute of Technology Atlanta, Georgia 30332	169
Dr. J. Richard Williams Nuclear Engineering Department Georgia Institute of Technology Atlanta, Georgia 30332	170
Dr. Glenn A. Greathouse P. O. Box 332 Ormond Beach, Florida 32074	171
Dr. Peter Chiarulli Head, Mechanics Department Illinois Institute of Technology Chicago, Illinois 60616	172
Dr. Andrew Fejer Head, Mechanical & Aerospace Engineering Department Illinois Institute of Technology Chicago, Illinois 60616	173
Dr. Zalman Lavan Illinois Institute of Technology M.A. E. Department Technology Center Chicago, Illinois 60616	174
Dr. T. P. Torda Illinois Institute of Technology M.A. E. Department Technology Center Chicago, Illinois 60616	175
Dr. Herbert Weinstein Chemical Engineering Department Illinois Institute of Technology Chicago, Illinois 60616	176

	Copy No.
Dr. B. D. Goracke Massachusetts Institute of Technology Aeronautics & Astronautics Room 37-371 Cambridge, Massachusetts 02139	177
Professor Elias P. Gyftopoulos Room 24-109 Massachusetts Institute of Technology Cambridge, Massachusetts 02139	178
Dr. A. Javan Massachusetts Institute of Technology Cambridge, Massachusetts 02139	179
Professor J. L. Kerrebrock Room 33-115 Massachusetts Institute of Technology Cambridge, Massachusetts 02139	180
Dr. W. S. Lewellen Room 33-119 Massachusetts Institute of Technology Cambridge, Massachusetts 02139	181
Professor Edward Mason Room NW12 Massachusetts Institute of Technology Cambridge, Massachusetts 02139	182
Dr. C. K. W. Tam Aeronautics & Astronautics Massachusetts Institute of Technology Room 37-371 Cambridge, Massachusetts 02139	183
Dr. Friedwardt Winterberg Nevada Southern University Professor of Physics Director of Laboratory for Space Research Desert Research Institute Las Vegas, Nevada 89109	184

	Copy No.
Dr. H. A. Hassan Department of Mechanical Engineering North Carolina State University Raleigh, North Carolina 27607	185
Dr. H. E. Unger Technological Institute Engineering Sciences Northwestern University Evanston, Illinois 60201	186
Professor E. P. Wigner Department of Physics Princeton University Princeton, New Jersey 08540	187
Dr. Bruce A. Reese, Director Jet Propulsion Center Mechanical Engineering Department Purdue University Lafayette, Indiana 47907	188
Professor M. J. Zucrow Atkins Professor of Engineering Mechanical Engineering Department Purdue University Lafayette, Indiana 49707	189
Mr. H. J. Ramm 606 Larrymore Drive Manchester, Tennessee 37355	190
Professor C. N. Shen Rensselaer Polytechnic Institute Troy, New York	191
Dr. W. H. Bostick Stevens Institute of Technology Hoboken, New Jersey 07030	192
Dr. A. V. Grosse Research Institute of Temple University 4150 Henry Avenue Philadelphia, Pennsylvania 19144	193

	Copy No.
Dr. George Nelson University of Arizona Nuclear Engineering Department Tucson, Arizona 85721	194
Professor H. C. Perkins Energy, Mass & Momentum Transfer Laboratory Aerospace & Mechanical Engineering Department University of Arizona Tucson, Arizona 85721	195
Dr. Paul T. Bauer Research Institute University of Dayton 300 College Park Dayton, Ohio 45409	196
Professor Ron Dalton Department of Nuclear Engineering University of Florida Gainesville, Florida 32601	197
Dr. D. Keefer Aerospace Engineering Department Department of Nuclear Engineering Sciences University of Florida Gainesville, Florida 32601	198
Dr. M. J. Ohanian Department of Nuclear Engineering Sciences University of Florida Gainesville, Florida 32601	199
Professor Rafael Perez Nuclear Engineering Department University of Florida Gainesville, Florida 32601	200
Dr. Richard T. Schneider 202 Nuclear Sciences Building Department of Nuclear Engineering Sciences University of Florida Gainesville, Florida 32601	201

	Copy No.
Professor Glen J. Schoessow Department of Nuclear Engineering Sciences 202 Nuclear Sciences Building University of Florida Gainesville, Florida 32601	202
Dr. Robert Uhrig Chairman, Department of Nuclear Engineering University of Florida Gainesville, Florida 32601	203
Dr. T. Ganley College of Engineering University of Illinois Urbana, Illinois 61801	204
Dr. G. C. Guyot College of Engineering University of Illinois Urbana, Illinois 61801	205
Mr. Paul E. Thiess Direct Energy Conversion Nuclear Engineering Program University of Illinois Urbana, Illinois 61801	206
Dr. J. T. Verden Gaseous Electronic Lab University of Illinois Urbana, Illinois 61801	207
Dr. K. Almenas Department of Chemical Engineering University of Maryland College Park, Maryland 20742	208
Dr. D. Tidman Institute for Fluid Mechanics University of Maryland College Park, Maryland 20742	209

	Copy No.
Dr. T. D. Wilkerson Institute for Fluid Dynamics and Applied Mathematics University of Maryland College Park, Maryland 20742	210
Dr. J. N. Davidson University of Michigan Ann Arbor, Michigan 48103	211
Dr. D. H. Timmons Nuclear Engineering Program University of Missouri Columbia, Missouri 65201	212
Mr. L. H. Bettenhausen Department of Nuclear Engineering Reactor Facility University of Virginia Charlottesville, Virginia 22901	213

UNITED AIRCRAFT CORPORATION